UNIVERSITY OF CALIFORNIA SAN DIEGO

Peripheral Neuropathy and Sexual Dimorphism in Prion Disease Mouse Models

A Thesis submitted in partial satisfaction of the requirements for the degree

Master of Science

in

Biology

by

Annee Dac Nguyen

Committee in charge:

Professor Nigel Calcutt, Chair
Professor Brenda Bloodgood, Co-Chair
Professor Sam Pfaff
Professor Christina Sigurdson
Professor Yimin Zou

2018

The Thesis of Annee Dac Nguyen is approved, and it is acceptable in quality and form for publication on microfilm and electronically:

_____

_____

_____

_____

Chair

_____

Co-Chair

University of California San Diego

2018

DEDICATION

In recognition of his outstanding mentorship, his patience, and his guidance, I would like to firstly thank my advisor Dr. Nigel Calcutt for inspiring me as a scientist, for teaching me to write, and for encouraging me to take calculated risks without compromising my integrity.

In recognition of their patience and their continued excitement regarding my scientific achievements throughout the year, I would like to thank my committee, Dr. Christina Sigurdson, Dr. Brenda Bloodgood, Dr. Sam Pfaff, and Dr. Yimin Zou.

To all my friends, my co-workers, and my loving significant other Aden, I thank you all for your support. This year has been a marathon, and it has meant the world to me that you all have helped to drag me towards the finish line.

Thank you all for teaching me that science is about storytelling, exploring endless possibilities, and learning to appreciate unexpected outcomes.

TABLE OF CONTENTS

SIGNATURE PAGE……iii
DEDICATION iv
TABLE OF CONTENTS……...v
LIST OF FIGURES vii
ACKNOWLEDGEMENTS viii
ABSTRACT OF THE THESIS ix
INTRODUCTION 1
Prion Disease 1
I. History 1
II. Types of Prion Diseases 2
III. Prion Structure 9
IV. Prion Disease Animal Models & Mutations 10
Peripheral Neuropathy 12
I. Peripheral Nerve: Structure & Function 12
II. Overview of Peripheral Neuropathy 13
III. Types of Peripheral Neuropathy & Common Phenotypes 14
IV. Peripheral Neuropathy in Prion Disease 15
METHODS 16
Animals 16
Behavioral Tests 17
I. Large Fiber Function 17
II. Small Fiber Function 18
Histological Analyses 20
I. Corneal confocal microscopy 20
II. Foot skin microscopy 22
III. Axonal caliber and myelin sheath area analysis 23
IV. Statistical analysis 24
RESULTS 24
Barbering and Fighting Behaviors 24
General Health 25
Small Fiber Function 27
Small Fiber Structure 28

Large Fiber Function 30
Large Fiber Structure 35
DISCUSSION 36
Peripheral Neuropathy in Prion Disease 36
Our Models of Prion Disease 36
Large Fiber Motor Neuropathy 37
Large Fiber Sensory Dysfunction & Sexual Dimorphism 39
No marked sensorimotor coordination deficits that would impact behavioral assays 40
Small fiber sensory dysfunction without change in small fiber structure 41
Prion Protein Deposition and Neuropathy 42
Sexual Dimorphism in Neurodegenerative Diseases 43
Summary & Future Studies 44
REFERENCES 46

LIST OF FIGURES

Figure 1. Linear calibration curve for thermal nociception test. 19

Figure 2. Corneal confocal microscopy images of sub-basal nerve plexus 21

Figure 3. Corneal confocal microscopy images of stromal layer 22

Figure 4. Graphic depiction of a myelinated axon. 24

Figure 5. Terminal body weight and rotorod testing of general sensorimotor function. 25

Figure 6. Latency of paw withdrawal response to thermal stimuli. 27

Figure 7. Small fiber density in left mouse foot skin and mouse eyes. 28

Figure 8. Large fiber function analysis: von Frey filament testing and MNCV measurements 30

Figure 9. Large fiber structure analysis of mice sciatic nerves. 32

ACKNOWLEDGEMENTS

I would like to acknowledge Professor Christina Sigurdson for providing me with transgenic prion mice and allowing me to include unpublished data in my introduction and my discussion regarding her novel transgenic 93N mouse model from her laboratory.

ABSTRACT OF THE THESIS

Peripheral Neuropathy and Sexual Dimorphism in Prion Disease Mouse Models

by

Annee Dac Nguyen

Master of Science in Biology

University of California San Diego, 2018

Professor Nigel Calcutt, Chair

Professor Brenda Bloodgood, Co-Chair

In this study, I characterize peripheral neuropathic phenotypes in F35 mice (knock-out model of prion disease) and 93N mice (novel knock-in model of prion disease) using various behavioral assays, electrophysiology, and histology. F35 mice and 93N mice show significant impairment of small unmyelinated C-fibers without systemic loss of nerve density in either the foot skins or the cornea. In analyzing large fiber function, F35 mice and 93N mice show significant slowing of motor nerve conduction velocity. However, only 93N male mice show significant impairment in large sensory nerve fiber function, suggesting a model- and sex-specific peripheral neuropathic phenotype in the knock-in model. Structural analysis of axon caliber distribution in sciatic nerves show significantly smaller mean axonal diameter in diseased mice, but no difference in total amount of large myelinated fibers. Overall, axonal size-frequency in sciatic nerves of diseased mice appear heavily skewed toward smaller nerve fibers. Analysis of myelin sheath g-ratio show thinner axon diameters in only F35 mice compared to wild type mice, but post-hoc analysis of only male mice shows that F35 and 93N males both have smaller axonal diameters compared to wild types. The presence of peripheral nerve pathology in both mice despite a lack of prion aggregates

in the central nervous systems of both mouse models suggests that prion aggregates may not be necessary to activate prion neurotoxic pathways.

INTRODUCTION

Prion Disease

I. History

Prion disease was first documented in the 1700s among herds of sheep (Journal of the House of Commons, 1775). The affected sheep would scrape themselves, a pathological behavior that caused the first known instance of prion disease to be called "scrapie." In the late 1800s, most causative agents of disease were determined to be viruses and bacteria, although the causative agent of scrapie remained unknown. It was initially proposed that scrapie in the sheep population was caused by a virus due to the disease's slow incubation period (Sigurdsson, 1954), although experiments to prove the viral inoculation theory were unsuccessful.

The first case of human prion disease, Creutzfeldt-Jakob disease (CJD), was documented in the early 1900s (Meggendorfer, 1930; Gambetti et al., 2003). Approximately fifty years later, a neurological disorder with similar clinical presentations to CJD and scrapie called kuru was described on the island of Papua New Guinea in the Fore Tribe of Papua New Guinea. Kuru appeared concentrated in the women and children of the tribe and seemed to spread among the tribe members via their endocannibalistic ritual. As kuru, scrapie and CJD revealed distinctive patterns of neurodegeneration such as vacuolation and similar mechanisms of transmission, they were determined to be from the same family of disease (Hadlow, 1959; Klatzo et al., 1959). These speculations were confirmed when two separate experiments reported that inoculation with brain matter from patients who succumbed to kuru and CJD resulted in fatal encephalopathy on both accounts (Gibbs et al., 1968; Beck et al., 1969).

Despite forming connections between these diseases of transmissible encephalopathy and discovering the mode of transmission, the infectious particle responsible was still unknown. One of the prevailing theories still was that kuru and CJD were caused by a slow viral infection (Sigurdsson, 1954). Another theory discovered a gene required to cause scrapie infection and dictated scrapie incubation time, which suggested that DNA was the transmissible infectious particle (Dickinson, Meikle, and Fraser, 1968). Further investigations of the infectious agent, however, found that the agent was likely not a nucleic acid, as it survived UV radiation, extreme temperatures, formalin, nucleases, and other factors that would denature or inactivate nucleic acids, viruses, and bacteria (Hunter and Millson, 1964; Pattison, 1965; Alper et al., 1967). Furthermore, the size of the infectious agent was determined to be too small to be a virus

or a bacterium (Alper et al., 1966). In 1967, scrapie infection was proposed to be caused by a proteinaceous particle, a controversial proposal as only bacteria and viruses were considered to be infectious agents (Griffith, 1967). The infectious protein or 'prion' narrative was further supported by experiments showing successful inactivation of the particle via methods that inactivated other proteins and isolating infectious protein aggregates from infected animals (*Pruisner et al.,* 1982, 1983).

To further investigate the genesis of the infectious particle, a study noted the mutant prion to be a derivative of a normal, pre-existing cellular protein within the host due to a lack of an immune response to infection (Pruisner et al., 1993). The cellular prion protein itself and the gene encoding it (*Prnp*) was also required to be present for infection to occur, as native prion (PrP^C) deficient and Prnp knock-out mice were resistant to infection via mutant prion inoculation (Oesch et al., 1985; Bueler et al., 1993). After several in vitro and in vivo experiments that generated mutant prions from host-recombinant prion proteins (Deleault et al., 2005; Barria et al., 2009; Zhang et al., 2013), the generally accepted mechanism of mutant prion formation was a misfolding of the normal, host prion protein, which resulted in a pathological prion that caused prion disease.

II. Types of Prion Diseases

Prion diseases are formally termed transmissible spongiform encephalopathies (TSEs). Any animal with tissue that expresses prion protein is vulnerable to contracting prion disease, as native prions are required for disease initiation to occur (Oesch et al., 1985). The most prominent populations affected by prion disease are humans and domesticated herd animals such as goats, sheep and cows, along with deer, and mink (McGowan, 1992; Marsh, 1992; William and Young, 1980; Wells et al., 1987; Trevitt and Singh, 2003).

Prion diseases are classified as acquired, sporadic, or familial. Most cases (85% to 90%) are sporadic or acquired. While sporadic cases have no clear external cause, prion disease can be acquired if one is exposed to mutant prion proteins via oral, surgical, or intravenous routes. Approximately 10% to 15% of prion disease cases are familial disorders caused by an autosomal dominant mutation of the prion protein gene, PRNP (Brown and Mastrianni, 2010). Common histopathologies of prion disease are astrogliosis, accumulation of protein aggregates, vacuolation of nervous tissue, and the formation of spongiform tissue (Brown and Mastrianni, 2010). The most common pathological behavioral traits are aggression, dementia, and loss of sensorimotor coordination (Imran and Mahmood, 2011; Thompson et al., 2014).

The common forms of prion disease are:

a. Scrapie

Scrapie was the first documented instance of prion disease and was discovered in sheep and goats. The name scrapie derives from the pathological behavior, in which animals scraped themselves against fences, suggesting pruritus. Other clinical signs of scrapie in sheep and goats include anxious behavior, tremors, unexplained weight loss, hunched posture, and teeth grinding (Capucchio et al., 2001; Konold et al., 2007). While scrapie-inducing prions are of unknown origin and have an incubation period of 2-5 years, infected animals die approximately 2 weeks to 6 months after clinical symptoms appear (Jeffrey and Gonzalez, 2007). Scrapie prions propagate to the nervous system, throughout most of the gastrointestinal system, lymph nodes, and most muscles throughout the body and lining major viscera (Maddison et al., 2010; O'Rourke et al., 2011). Because scrapie prions are also concentrated in bodily excretions and secretions, exposure to infected excretions has been proposed as a possible mode of transmission within a flock (Mabbott, 2017).

Native prion protein exists in multiple polymorphisms. The most scrapie susceptible polymorphisms identified in the prion gene are 136V (valine at codon 136); 154R (arginine at codon 154); and 171Q (glutamine at codon 171) (Baylis et al., 2004; Imran and Mahmood, 2011). To decrease the incidence of scrapie among domesticated sheep and goats, Prnp polymorphisms associated with low-risk susceptibility to scrapie (such as 136A) have been artificially selected for in breeding new flocks of sheep and goats (Goldmann, 2008, Trevitt and Singh, 2003). Despite selecting for low-risk polymorphisms, sheep and goat are still vulnerable to a sporadic form of scrapie called 'atypical scrapie,' and are thus not entirely scrapie-risk free (Benestad et al., 2008).

Several animal models have been developed to characterize scrapie. These include transgenic mice such as Tga20 mice, which overexpress wild-type murine PrP^c, and mice with inoculated prions from bank voles; goats and sheep; and macaques (Cuille and Chelle, 1939; Pattison, 1966; Chandler, 1961; Gibbs, 1972; Fischer et al., 1996; Haybaeck, 2011; Sigurdson et al., 2012; Watts, 2014; Cornoy, 2015). The most common mouse-adapted scrapie prion mutants examined in these models are the RML (also called the Chandler strain), ME7, 139A, and 79A strains. Each of these strains differ by their respective concentrations of mono-, di-, and unglycosylated prion proteins (Thackray et al., 2007; Bradner and Jaunmuktane, 2017).

b. Bovine Spongiform Encephalopathy (BSE)

Bovine spongiform encephalopathy (BSE) is a fatal neurodegenerative disorder in cattle that was first documented in the United Kingdom in the mid-1980s. Because it affected cattle in the food production industry and was transmittable to other species, BSE threatened global food supply and endangered the public health of humans, domesticated animals, and zoo animals. During the height of the United Kingdom's BSE outbreak, 120,000 cattle were diagnosed with BSE in the UK and 200,000 cattle were subsequently slaughtered across Europe to prevent human consumption (*Center for Food and Safety*, 2018, Torres et al., 2011). The presumed cause of BSE was farm feed containing meat and bone from other animals infected by scrapie protein from sheep. This speculation was supported after a ban in meat and bone feed led to a subsequent decrease in BSE incidents (Ducrot et al., 2008).

An alternative theory proposed that BSE prions are a separate family of proteins from the scrapie protein with their own unique mutations and structures. Studies supporting a spontaneous BSE prion protein have identified a mutation in the bovine *Prnp* gene that causes a genetic predisposition to BSE (Richt and Hall, 2008). Moreover, studies found two distinct prion forms of BSE, the L-type and H-type isoforms, in cattle populations across several countries (Yamakawa et al., 2003; Biacabe et al., 2004; Casalone et al., 2004; Jacobs et al., 2007; Richt et al., 2007). The L-type and H-type isoforms of BSE are termed 'atypical' or spontaneous BSE prions of lower molecular mass and higher molecular mass, respectively, compared to the classic, 'typical' BSE prion (Jacobs, et al., 2007).

BSE prions have an incubation period from 2 to 8. While BSE and scrapie prions are both found throughout the nervous system and parts of the gastrointestinal system, BSE proteins are also found in the bone marrow, adrenal glands, and tonsils, and are notably concentrated in peripheral nerves (Novakofski et al., 2005). The primary mutations that confer the most susceptibility to BSE are an E211K (glutamate to lysine substitution to codon 211) polymorphism and two insertion/deletions (indels) in the Prnp gene, one that is a 23-base pair indel in the promoter and another that is a 12-base pair indel in the first intron (Nicholson et al., 2008; Richt, 2008; Sander et al., 2004; Heaton et al., 2008; Juling et al., 2006). While the E211K polymorphism does not make up most BSE cases, it is interesting to note that the polymorphism is analogous to the mutation of familial Creutzfeldt-Jakob disease (E200K) (Heaton et al., 2008).

Several animal models of BSE have been developed in mice, sheep, marmosets and macaques via intracerebral, intraparietal, oral and intravenous inoculation (Lasmezas et al., 1996; Hill et al., 1997; Lasmezas et al., 2005; Watts et al., 2014, Lescoutra-Etchegaray, 2015). Key mouse models of BSE include mouse-adapted BSE prions with

polymorphisms 301C and 301V (Collinge and Clarke, 2007). Additionally, transgenic mice homozygous for methionine and/or valine at codon 129 of the human Prnp gene are highly susceptible to BSE prion inoculation (Asante, et al., 2002).

c. Creutzfeldt-Jakob Disease (CJD)

Creutzfeldt-Jakob disease (CJD) can be subclassified into variant CJD (vCJD), iatrogenic CJD (iCJD), sporadic CJD (sCJD), and familial CJD (fCJD). Of the four, vCJD and iCJD are the only two acquired forms of CJD. While the symptoms of CJD are heterogenous and unique for each individual, the main clinical feature of CJD is dyskinesia that can occur with or without muscular atrophy, cerebellar ataxia, insomnia, difficulty speaking, difficulty swallowing, and dementia. Most types of CJD appear to arise from methionine or valine polymorphisms at residue 129 on the Prnp allele (Moore et al., 2016). Genotypic combinations of polymorphisms at codon 129 include 129MM1, 129MV1, 129VV1, 129MM2, 129MV2, and 129VV2, in which 1 and 2 correspond to protease-resistant prion proteins type 1 PrP^{res} (unglycosylated prion with mass 21.5 kD) and type 2 PrP^{res} (unglycosylated prion with a mass of 19.4 kD) (Tranchant et al., 1999; Iwasaki, et al., 2006). Ratios of polymorphic heterozygotes and homozygotes vary for each subtype of CJD, and each variant contributes to the heterogeneity of phenotypes in CJD (Parchi et al., 1996; Trachant et al., 1999; Hauw et al., 2000; Iwasaki et al., 2006). There are four types of human mutant prions associated with sporadic and acquired CJDs. Types 1 and 4 are associated with 129MM1 and 129MM2, type 3 is associated with any polymorphism of 129V, and type 2 can be associated with any polymorphism genotype (Collinge et al., 1996).

i. Sporadic CJD (sCJD)

Sporadic CJD (sCJD) accounts for approximately 85% of disease incidences (Trevitt and Singh, 2003). sCJD is a late-onset neurodegenerative disorder and affected patients die within about six months after clinical symptoms are present. Clinical symptoms of sCJD include hallucinations and visual disturbances, cerebellar ataxia, and rapid progression of dementia (Cornelius, et al., 2009). sCJD cases occur globally, do not appear to be caused by exposure to external scrapie proteins and do not show hereditary patterns (Brown et al., 1987; Wadsworth et al., 2001). Current theories suggest individuals with polymorphisms at codon 129 of the Prnp alleles are more susceptible to sCJD. sCJD can be caused by the following polymorphisms at codon 129 of the Prnp alleles: MM1/MV1, VV1, MM2, MV2, and VV2 (Parchi, et al., 1996; Gambetti, et al., 2003). sCJD heterozygotes have less severe clinical manifestations than

sCJD homozygotes, with a later age of onset and longer disease progression that is similar to vCJD (between 9 and 35 months) (Baker et al., 1991; Hill et al., 1999).

ii. Variant CJD (vCJD)

Variant Creutzfeldt-Jakob disease (vCJD) is an acquired form of prion disease contracted from ingesting tissue infected with bovine spongiform encephalopathy (BSE) (Bruce et al., 1997). vCJD first emerged in the mid-1990s amid the BSE outbreak among cattle in the United Kingdom. People who ingested BSE-infected tissue were subsequently infected. Although vCJD accounts for approximately less than 1% of known prion disease incidences, vCJD is the only prion disease that has significantly increased in incidence (by 23% per year) since 1994 and has infected roughly 200,000 people in the UK (Anderson et al., 1996; Andrews et al., 2000). vCJD has a mean age of onset around 29 years of age, a longer incubation time than sporadic CJD, and a clinical course between 9 and 35 months (Will et al., 1996). vCJD differs from sCJD by its slower clinical progression, increased amyloid beta plaques in brain tissue, presence of mutant protein in more tissue types than sCJD, and a heterogeneous incidence that is concentrated in areas of known BSE outbreaks (Will et al., 1996; Wadsworth et al., 2001). The transgenic mouse model homozygous for methionine at codon 129 of the human Prnp gene (129MM) is also a model for vCJD and this polymorphism is associated with a majority of clinical vCJD cases (*National CJD Research and Surveillance Unit,* 2017). While the 129MM polymorphism is characteristic of both vCJD and sCJD, the vCJD prion is shown to have a conserved proteolytic cleavage site that is unaffected by its glycosylation state and is noted to be a type 4 PrP^{Sc} (Collinge et al., 1996).

iii. Iatrogenic CJD (iCJD)

Iatrogenic Creutzfeldt-Jakob disease (iCJD) is an acquired form of prion disease, usually transmitted via a medical procedure such as using surgical tools contaminated with biological material containing mutant prion proteins from an infected person. As with vCJD, iCJD accounts for approximately less than 1% of known prion disease incidences (Trevitt and Singh, 2003). Prions are extremely resistant to standard sterilization procedures and can thus be spread via infected surgical instruments. iCJD can therefore unwittingly contribute to the spread of vCJD and other prion diseases. While prions must enter the body through an incision or be ingested to infect the body, important surgical procedures such as blood transfusions, organ transplants, and tissue grafts are complicated by the additional concern of the spread of prion disease, as prions are widely distributed in the body (Fleschsig et al., 2001; Bosch, 2001;

Wadsworth et al., 2001). Additionally, iCJD can also spread between species, (Gravenor et al., 2000). The 129 MM homozygous polymorphism is a risk factor for susceptibility to iCJD, as in sCJD, which may explain the similar range of clinical symptoms between iCJD and sCJD (Imran and Mahmood, 2011).

d. Familial Prion Diseases

Familial forms of prion disease are autosomal dominant disorders and account for approximately 10% to 15% of prion disease cases (*National CJD Research and Surveillance Unit,* 2017). Genetic forms of prion disease have more than fifty-five identified corresponding mutations of the Prnp allele (Kong et al., 2004). Familial prion diseases include familial Creutzfeldt-Jakob disease (fCJD), fatal familial insomnia (FFI), and Gerstmann-Straussler-Scheinker syndrome (GSS), each of which is described below:

i. Familial Creutzfeldt-Jakob disease (fCJD)

Familial Creutzfeldt-Jakob disease (fCJD) accounts for approximately 5% to 15% of all prion disease cases. The progression of clinical symptoms in fCJD first begin with confusion and memory impairment and proceed to cerebellar ataxia and myoclonus. Disease onset usually occurs between 30 and 50 years of age, although onset can occur as late as 80 years of age. fCJD is most commonly caused by inherited point mutations of the Prnp gene. Risk factors for fCJD includes the presence of indels within PrP from residues 51-91 and codon 129 genotypes on the Prnp alleles (Imran and Mahmood, 2011). Known mutations of fCJD are E200K, I210V, D128N, and V180I (Nozaki et al., 2010; Gambetti et al., 2011). Unlike other prion diseases, fCJD has little expression of unglycosylated fragments (Capellari et al., 2011).

ii. Fatal Familial Insomnia (FFI)

Previously known as thalamic dementia, fatal familial insomnia (FFI)'s main neuropathological feature involves the selective neurodegeneration of thalamic nuclei with little mutant prion protein deposition. The key linked mutations associated with FFI is a haplotype mutation of a Prnp allele mutation (D178N) and the methionine of the Prnp polymorphism M129V, although the D178N mutation can also be linked to a valine of the M129V Prnp polymorphism (Lugaresi et al., 1986 Montagna et al., 2003). The inheritance pattern of FFI of 129MM genotypes and 129MV genotypes is gender-independent and the mean age of onset is 49 years of age, although onset spans from 20 to 72 years of age. Affected patients die after an average of approximately 18 months, although survival time after onset of disease can range from 8 to 72 months. Patients with the 129MM genotype have shorter survival time and increased severity of clinical symptoms. Hallmark symptoms of FFI include insomnia, myoclonus (muscle spasms), insomnia-induced hallucinations, autonomic dysfunction, cerebellar ataxia and seizures (Belay, 1999; Brandel, 2004; Capellari et al., 2011; Montagna et al., 2003).

The most relevant mouse model of FFI expresses a mouse-adapted prion protein with linked mutation D177N/M128, which is homologous to the human FFI mutation described above. The mutant mouse prion protein is insoluble in the brain, mildly protease-resistant, and has a molecular mass of approximately 19 kD, which is similar to that of human FFI prions (Monari et al., 1994; Dossena et al., 2008; Bouybayoune et al., 2015).

iii. Gerstmann-Straussler-Scheinker syndrome (GSS)

The general neuropathological features of Gerstmann-Straussler-Scheinker syndrome (GSS) are abundant amyloid plaques, neuronal loss, astrogliosis, neurofibrillary tangles, and variable severity in spongiform changes.

GSS is an early-onset familial disorder that exhibits the slowest disease progression of all familial disorders, with survival time ranging from 3 years to 10 years post-disease onset. The most common symptoms in GSS patients are cerebellar ataxia, dementia, dysarthria (difficulty speaking), spasms, gait abnormalities, and leg hypoflexia (below normal reflexes) or areflexia (loss of reflex) (Belay, 1999; Brandel, 2004). As with the other prion diseases, the M129V polymorphism linked to the various GSS-associated mutations affects the range of disease phenotypes (Bianca et al., 2003). Of the many GSS-related mutations, the only reproducible and two most common mutations in GSS mouse models are the A116V mutation (homologous to the human A117V mutation) and the P102L mutation (Yang et al., 2010; Umeh et al., 2016).

III. Prion Structure

Each type of prion disease has a signature abnormal conformation of the host prion protein and is differentiated from the others by molecular masses and number of types of attached glycoproteins (Torres et al., 2011). The native, host-encoded prion protein is a glycoprotein consisting of approximately 210 amino acids that is anchored in the plasma membrane via a C-terminal glycophosphatidylinositol (GPI) (Pruisner, 1998; Weissman, 2004). The function(s) of native prion protein remain relatively unclear, with theories ranging from cell-cell communication, prevention of apoptosis and oxidative stress, and participation in synaptic function regulation (Caughey and Baron, 2006; Watts and Westaway, 2007). Because prion diseases are caused by misfolding of host-encoded prion proteins, studying mutations of the prion protein structure can aid in identifying key structures that may be relevant to both prion neurotoxicity and further characterization of the host-encoded prion's function.

a. C-terminus

The C-terminus of the prion protein, also known as the globular domain (residues 126-230 of PrP), is structurally conserved across most species and contains two beta strands and three alpha helices (Zahn et al., 2000). Within the C-terminal are two N-glycosylation sites, a gamma cleavage site, a disulfide bridge, and a glycosylphosphatidylinositol (GPI) anchor (Stahl et al., 1987, 1992).

The globular domain contributes to the stability of the prion protein, endoplasmic reticulum (ER) processing of the prion, and regulation of prion neurotoxicity mechanisms (Gambetti, 2003; Heske et al., 2003; Jackson et al., 2013; Wu et al., 2017). In most human prion diseases, the C-terminal core of mutant prion aggregates is resistant to proteinase K (PK) digestion, and protein aggregates develop prior to spongiform degeneration in the same nervous

tissue (Gambetti, 2003; Jackson et al., 2013). Other mouse-adapted prion models with truncated C-terminal domains such as W144Stop and Q159Stop are not successfully imported into the endoplasmic reticulum, cannot undergo N-terminal processing, are unable to anchor themselves to neuronal plasma membranes, and are digestible by PK (Heske et al., 2003). The key role of the C-terminus is to modulate the N-terminus neurotoxicity through direct contact (Wu et al., 2017).

b. N-terminus

While the C-terminal is always folded, the N-terminus of the protein is modified depending on the species, usually with at least four octapeptide repeats that are abundant in glycine and can bind to a multitude of divalent ions (Wuthrich and Riek, 2001; Millhauser, 2004; Choi et al., 2006). Other domains within the N-terminal are two charge clusters, CC1 and CC2, and a hydrophobic domain. Alpha and beta cleavage sites flank both sides of charge cluster CC2 (Harris et al., 1993).

As the N-terminus contains both alpha and beta cleavage sites, the N-terminus is hypothesized to be a neurotoxic factor in prion disease that induces oxidative stress (Sonati et al., 2013; Wu et al., 2017). Normally, alpha cleavage creates CC1 fragments and prevents conversion of PrP to PrP^{Sc}. However, in prion disease, beta cleavage is upregulated and prion models with deleted N-terminus-related alpha cleavage sites exhibit spontaneous neurodegeneration (Chen et al., 1995; Westergard et al., 2011). The N-terminus also contains a short, polybasic region from residues 23 to 31 that aids the host-encoded prion protein to bind to scrapie proteins and induce prion propagation (Turnbaugh et al., 2012). Because the N-terminus appears to be the neurotoxic effector of the prion protein, many animal models have been used to further characterize N-terminus structure and function in relation to the native prion protein.

IV. Prion Disease Animal Models & Mutations

Animal models of prion disease include mice with knock-out or knock-in mutations to the *Prnp* allele, which can result in indel mutation or amino acid substitutions in the prion protein. Animal models of prion disease have been used to identify the function of each domain of the prion protein, the function of the host-encoded prion protein and the mechanism of prion propagation and infection. An early study using null *Prnp* knock-out mice (*Prnp* -/-) reported a complete resistance to prion infection in the absence of both *Prnp* alleles, suggesting that host-encoded proteins are required for prion infection and propagation (Bueler et al., 1993). Knock-out models of prion disease, in which

residues of the prion protein are deleted, show that several deletions of the host-encoded prion protein, such as deletions of residues 32-80, 32-121, 32-134, and 105-125, resulted in neurotoxicity with variable severity of phenotypes (Shmerling et al., 1998; Li et al., 2007).

Studies with knock-in mouse models also report that disease phenotypes from N-terminal deletions can be reversed by reintroducing either one *Prnp* allele or host-encoded prion proteins (Fischer et al., 1996; Shmerling et al., 1998; Bremer et al., 2013). Knock-in mouse models have also shown that octapeptide repeats insertions (OPRI) in the N-terminus can result in spontaneous neurodegeneration (Chiesa et al., 1998). Through prion disease animal models, the N-terminus has been identified as a primary neurotoxic effector of the mutant prion (Sonati et al., 2013). The study that I report in this thesis compares two animas models, one of which is a novel prion disease model, with an amino acid substitution in the 93rd residue of the N-terminus, and the other being an established mouse model of prion disease with deletions of residues 32-134 in the N-terminus. to explore further the N-terminus's role in prion neurotoxicity.

a. Transgenic F35 Knock-Out Mice

This knock-out model has a modified prion protein that is truncated at the N-terminus between residues 32 - 134. Transgenic F35 mice are a common mouse model in prion disease studies and have been used to characterize the functions of each domain of the prion protein. Studies characterizing F35 mice showed them to develop ataxia, tremors, hunched backs, and weight loss, with death occurring by around 80 days (Shmerling et al., 1998; Li et al., 2007). Hemizygous F35 mice with one wild type PrP allele do not develop clinical symptoms (Shmerling et al., 1998). Multiple studies investigating deletions in the N-terminus have determined that deletions could increase prion susceptibility, induce spontaneous neurodegeneration, and/or maintain prion propagation and transmission (Fischer et al., 1996; Schmerling et al., 1998; Flechsig et al., 2000; Baumann et al., 2007; Li et al., 2007; Solomon et al., 2010).

b. Transgenic 93N Knock-In Mice

The transgenic mouse model has an amino acid substitution of Q93N, with amino acid Q substituted for amino acid N at residue 93 in the N-terminus of the prion protein and N-linked glycans. Despite spontaneous neurodegeneration, formation of spongiform tissue, and astrogliosis in the hippocampus, no known prion protein aggregates have been observed in central nervous system tissue (Sigurdson Lab, Personal Communication, unpublished data). These findings suggest that prion protein aggregates may not be required to induce neurotoxicity and supports previous suggestions that the N-terminus is a neurotoxic effector of the prion protein.

Peripheral Neuropathy

I. Peripheral Nerve: Structure & Function

The peripheral nervous system consists of nerves and ganglia outside the brain and spinal cord. A nerve consists of the central endoneurium containing individual nerve fibers (neuronal axon + Schwann cell) and endoneurial blood vessels, that is bounded by a perineurial sheath and an epineurium of connective tissue. Nerves may contain a mixture of sensory nerve fibers and motor nerve fibers or only one type of fiber. Sensory nerve fibers, also known as primary afferent nerve fibers, relay nociceptive (painful) and nonpainful thermal and tactile stimuli from peripheral limbs and organs to the spinal cord and brain. Motor nerve fibers, or efferent nerve fibers, conduct impulses from the central nervous system towards the muscles to cause movement. Each peripheral nerve fiber consists of a neuron with a neuronal body (soma) and axon, plus a Schwann cells that may wrap the axons to form an insulating myelin sheath.

The myelin sheath facilitates electrical transmission down the peripheral nerve by decreasing capacitance and increasing electrical resistance along the axonal membrane. Because electrical impulses cannot depolarize segments of the axon that are surrounded by myelin sheaths, the impulses depolarize the exposed membrane at the nodes between myelin sheaths and proceed to jump from node to node (Morell and Quarrles, 1999). In the peripheral nervous system, myelin is formed around axons of diameters > 1μm (Taveggia, 2016). Myelin growth and axonal growth occur in tandem throughout nerve maturation. The ratio of the myelin sheath to the diameter of the axon remains constant across all axon sizes to optimize nerve conduction velocity. The optimal ratio of the axonal diameter to the myelinated fiber diameter (axon + myelin), or the g-ratio, is 0.6 in the peripheral nervous system (Chomiak and Hu., 2009; Barry et al., 2012).

G-ratios that differ from the optimal g-ratio value suggest peripheral nerve disease. Smaller g-ratio values could result from axonal diameter shrinkage or thicker myelination. Axonal diameter shrinkage is associated with slowing of nerve conduction velocity and has been shown to occur in rat models of chronic diabetic neuropathy (Gasser and Grundfest, 1939; Rushton, 1951; Sima et al., 1983; Jakobsen et al., 1983). Thicker myelination of small axons or tomacula has been reported in diseases such as autosomal recessive hypermyelinating neuropathy and peripheral myelin protein (Pmp22) deficient mouse models (Sabatelli et al., 1994; Adikofer et al., 1995). Larger g-ratio values relative to the optimal g-ratio value could arise from thinner myelin or axonal swelling. Thinner myelination occurs

in demyelinating polyneuropathies (Morelli et al., 2017). Axonal bulging has been reported in transgenic prion disease mouse models such as Tg(PG14) mice (Jeffrey et al., 2009).

The nodes of Ranvier are the gaps between adjacent Schwann cells and, if present, their myelin sheaths that are the only segments along the axon through which ion flow across the neuronal membrane occurs. Because myelinated axons allow for the action potential to jump from one node of Ranvier to another and span internodal distances, myelinated nerve fibers have faster nerve conduction velocities than unmyelinated nerve fibers (Ranvier, 1871). Conduction velocity of nerves increase as internodal distance increases, length of nodes increases, and the density of sodium channels at nodes of Ranvier increases (Waxman, 1975; Brill et al., 1977). In pathologies in which demyelination occurs, subsequent remyelination of the nerve fiber leads to shorter lengths of nodes of Ranvier and consequently, slower nerve conduction velocity (Villalon et al., 2018).

The structure of the synapse includes the synaptic cleft, synaptic terminals, and receptors on the preganglionic neuron and the postganglionic neuron. The synaptic terminals of peripheral neurons release neurotransmitters that cross the synaptic cleft to another receiving neuron's presynaptic terminals (Pavelka and Roth, 2010). Pathologies of the synapse can occur if exocytosis of neurotransmitters from the presynaptic terminal do not occur or if receptors of the postsynaptic terminals cannot bind or respond to neurotransmitters.

II. Overview of Peripheral Neuropathy

Pathologies of the peripheral nerves are known as peripheral neuropathies (PN). Peripheral neuropathies are frequently associated with neurodegenerative or metabolic disorders such as Alzheimer's disease, Parkinson's disease, human immunodeficiency virus (HIV), ALS, MS, diabetes, and obesity (Reichling and Levine, 2010). Because peripheral neuropathies affect many populations with pre-existing neurodegenerative disorders, around 20 million people in the United States alone suffer from some form of peripheral neuropathy (National Institute of Neurological Disorders and Stroke, 2018). Pathologies of sensory nerves and motor nerves occur when structures such as myelin sheaths, axons, and synaptic terminals are damaged, either by external stimuli or other neurodegenerative diseases. Damaged sensory nerves and motor nerves can fail to produce or release neurotransmitters, demyelinate or die, which can result in loss of sensation, aberrant sensorimotor coordination and inappropriate reaction to painful and nonpainful mechanical and thermal stimuli. More than 100 different types of peripheral neuropathies have been described and there are diverse clinical presentations.

III. Types of Peripheral Neuropathy & Common Phenotypes

a. Sensory neuropathy

Sensory neuropathies are peripheral neuropathies in which afferent nerves are impaired in either structure or function. In peripheral neuropathies, small and large sensory nerve fibers may become demyelinated, fail to release neurotransmitters or die.

Small sensory fibers, namely unmyelinated C-fibers and thinly myelinated Aδ-fibers respond to nociceptive thermal stimuli. Their primary neurotransmitters/hormones are substance P and glutamate. In the present study I have focused on small sensory fibers in the cornea and foot skin of the F35 and 93N mouse models. Studies using mouse models of diabetic peripheral neuropathy show that loss of nerve occupancy in the cornea and the foot skin is a hallmark of peripheral neuropathy. Common behavioral phenotypes of small sensory fiber pathology include thermal hyperalgesia and thermal hypoalgesia. Thermal hyperalgesia is hypersensitivity to painful thermal stimuli and is typical of early stages of peripheral neuropathy. Conversely, thermal hypoalgesia is hyposensitivity to painful thermal stimuli and is typical of later stages of peripheral neuropathy due to retraction or distal degeneration of the nerve fibers (Jensen and Finnerup, 2014).

Large myelinated sensory fibers respond to mechanical stimuli. Their primary neurotransmitter is acetylcholine. Approximately 23% to 48% of nerve fibers in the rat sciatic nerve are sensory nerve fibers (Schmalbruch, 1986). Pathologies of large sensory fibers produce phenotypes reflecting abnormal sensing of tactile stimuli, such as tactile allodynia and tactile hypoalgesia. Tactile allodynia is hypersensitivity to innocuous mechanical stimuli, whereas tactile hypoalgesia is hyposensitivity to mechanical stimuli (Jensen and Finnerup, 2014).

b. Motor neuropathy

Motor neuropathy describes peripheral neuropathies in which efferent nerves are impaired in either structure or function. In motor neuropathies, small and large motor nerve fibers may become demyelinated, fail to release neurotransmitters or die.

Dysfunction of large motor neurons in the sciatic nerve can lead to motor nerve conduction velocity (MNCV) slowing. MNCV slowing can be due to changes in myelin g-ratio caused by shrinking axonal diameter, demyelination of large fibers, or thicker myelination of the axon (Villalon et al., 2018). Other potential causes of MNCV slowing are changes in internodal distance, decrease in myelinated fiber density, or inability to release or

produce neurotransmitters (Waxman, 1975; Brill et al., 1977; Kambiz et al., 2015). As MNCV slowing is a hallmark of large fiber peripheral neuropathy, measuring MNCV is a standard procedure in evaluating peripheral neuropathy.

Motor neuropathy can also contribute to loss of coordination. A common procedure in peripheral neuropathy studies to test overall sensorimotor coordination using the rotarod behavioral assay. The merit of performing the rotarod assay is to ascertain that experimental animals do not have inhibited movements that would prevent them from performing other behavioral assays that identify peripheral neuropathic phenotypes.

IV. Peripheral Neuropathy in Prion Disease

While prion disease is considered a disease of the central nervous system, the peripheral nervous system aids in mutant protein propagation by acting as the primary pathway for prion CNS neuroinvasion (Crozet et al., 2007, Aguzzi et al., 2003) and is thus exposed to the neurotoxic properties of prions. Although prion disease-associated peripheral neuropathy has not be extensively documented in domesticated animals, studies with CJD patients report clinical symptoms of peripheral neuropathy, such as numbness and tingling in the extremities, as well as structural evidence of motor neuron disease, axonal disease, and axonal-demyelinating neuropathy (Neufield et al., 1992; Niewiadomska et al., 2002; Wang et al., 2018). In these studies, loss of sensation did not usually accompany axonal-demyelinating polyneuropathy in CJD patients. In a study of familial prion disease, a nonsense mutation, Y163X (which truncates the C-terminus such that the GPI membrane-anchoring tail does not exist) was reported to cause early-onset length-dependent sensory axonal peripheral neuropathy (Mead et al., 2014). Peripheral neuropathy in patients with the Y163X mutation presented much earlier than central nervous system neurodegeneration. Despite this clinical evidence, peripheral neuropathy has not been widely studied in experimental mouse models of prion disease. Peripheral neuropathy in mouse models of prion disease has been reported in both knockout and transgenic mice as a chronic demyelinating polyneuropathy. For example, in a study of PrP knockout mice, null mice experienced demyelinating polyneuropathy in the absence of host-encoded prion protein (Bremer et al., 2010). In a study with transgenic PrP mice, demyelinating neuropathy was reported in transgenic mice overexpressing host-encoded prion protein derived from Syrian hamsters (Westaway et al., 1994).

Specific Aims

In this study, I have characterized the peripheral neuropathic phenotype of F35 mice (a knock-out model of prion disease) and 93N mice (a novel knock-in model of prion disease) using various behavioral assays,

electrophysiology, and histology.

To test for motor neuropathy, I measured motor nerve conduction velocity in the sciatic nerves of F35 and 93N mice and compared them to MNCV of control mice. To identify potential causes of MNCV slowing, I evaluated multiple indices of large myelinated fiber structure such as g-ratio, total number of myelinated fibers per sciatic nerve, mean axonal diameter and overall size-frequency distribution of axonal caliber in each mouse model.

To test for sensory neuropathy, I evaluated paw withdrawal behaviors in response to noxious thermal stimuli and mechanical stimuli using the thermal nociception test and von Frey filament testing, respectively. To ensure that paw withdrawal behaviors are not hindered by sensorimotor coordination deficits, I performed rotarod testing to assess motor coordination of F35 and 93N mice. To determine if potential sensory nerve dysfunction corresponds to nerve structural deficits, I analyzed nerve occupancy of small sensory fibers in the cornea and foot skin.

My key findings were that both F35 mice and 93N mice showed significant dysfunction in small sensory fibers and large motor fibers, with large sensory fiber dysfunction only in 93N males. Small sensory fiber and large motor fiber dysfunction did not show corresponding loss of nerve fiber density in the foot skin or the sciatic nerve, respectively. However, large fibers in the sciatic nerve showed shrinkage of mean axonal diameter. While only the g-ratio of F35 mice was significantly lower than that of control mice, exploratory post-hoc analysis of only male mice showed that F35 and 93N male mice had significantly lower g-ratios than control mice. Overall, these findings suggest that peripheral neuropathy in N-terminus-modified F35 and 93N mice may result from axonal dystrophy and may be sex-specific in the novel 93N model.

METHODS

Animals

Three strains of mice were provided by Dr. Christina Sigurdson, DVM, PhD, of the Department of Pathology at UCSD School of Medicine. Control mice provided were three wild-type C57BL/6NJ males, denoted in this study as C57 mice. The two prion disease mouse models that were compared were F35/BL6 x KO mice, abbreviated as F35 mice, and 93N x 93N mice, abbreviated as 93N mice. The F35 group had two female mice and four male mice. The 93N mice had four female mice and three male mice. Mice were weighed weekly, and terminal weights were collected at the end of eight weeks prior to tissue collection.

Behavioral Tests

All behavioral tests performed to test large fiber and small fiber function were performed at baseline, four weeks, and terminal eight weeks. For von Frey filament testing, rotarod, and thermal nociception testing, animals were coded and randomized to perform double-blinded trials.

I. Large Fiber Function

a. Von Frey Filament Testing

To measure sensitivity to mechanical stimuli and assess large fiber function, von Frey filament testing was used. Von Frey filaments had a range of grams of force from 0.16 gram to 6.0 grams (filaments 3.22 (0.16 g), 3.61 (0.4 g), 3.84 (0.6 g), 4.08 (1.0 g), 4.31 (2.0 g), 4.56 (4.0 g), and 4.74 (6.0 g)) (Best Priced Products, White Plains, New York). Mice were placed upon a self-constructed, mesh metal panel upon a stand inside of glass beakers as restraint chambers and left to acclimate for a minimum of fifteen minutes prior to testing.

Testing began with starting filament 3.84. Filaments were applied at the plantar surface of each mouse paw and were pressed into the paw five times, once per second, for a total of five seconds. The filament should never leave the plantar surface of the paw during testing unless the mouse reacts. Mice should not be tested while they are urinating, grooming, or rearing. During testing, mice were observed for hind paw withdrawal response, such as flinching, withdrawing the paw, and or licking the paw. Both left and right paws were tested. All mice should be tested on one paw prior to testing on the other paw. 50% paw withdrawal thresholds of force (in grams) were calculated using a von Frey calculator and used in statistical analysis.

b. Motor Nerve Conduction Velocity (MNCV)

To measure function of sensory and motor nerves in large nerve fibers, motor nerve conduction velocity tests were conducted. Animals were first placed in an anesthesia induction chamber. Then, anesthesia was administered to animals as a mixture of 2.5 to 4 ppm of isoflurane with oxygen. Once anesthetized, animals were placed upon a heated metal pad warmed by a water heater. The set up of the anesthesia chamber with the isoflurane regulator and delivery system connected with the heated metal pad and water heater was from Braintree Scientific Inc. (Braintree Scientific Inc., Cat #: EZ-7150).

To monitor individual animals' temperatures, a thermistor probe attached to a temperature controller was inserted into the mice's anuses (Yellow Springs Instruments model 73ATC). Mice were then covered with a Kimwipe to prevent exposure to excess heat and were heated with a mobile hand lamp until their body temperatures were to 37°C. Individual animal temperatures and anesthetic dosages were monitored so that the nerve was consistently at 37°C.

To measure the MNCV of each animal, platinum tipped sub-dermal needle electrodes were used: a grounding electrode, two recording electrodes, and one stimulating electrode (Grass Technologies, Cat #: F-E2). The grounding electrode was placed in the scruff of the neck, the two recording electrodes were placed on either side of the second and third digits of the paw, and the stimulating electrode alternated between the Achilles heel and the notch of the hip. Only the left side of each animal was measured. Three pairs of alternating measurements between the tendon of the Achilles heel and the notch of the hip were taken**.** The difference between the H waves or M waves are calculated for each of the three pairs of measurements to derive three measurements of latencies. The length between each animal's Achilles heel and the notch of the hip were measured using a caliper**.** To calculate the MNCV, the length between the heel and the notch is divided by the median latency of the three pairs of calculations derived from the H waves or M waves (shown by the equation below).

$$MNCV\left(\frac{m}{\text{sec}}\right) = \frac{length\ of heel\ to\ notch\ (mm)}{median\ latency\ (msec)}$$

II. Small Fiber Function

a. Thermal Response Testing

To measure the temperature at which the mice react to gradually increasing thermal stimuli, thermal response testing was conducted on both paws of each mouse, using thermal nociception testing device (UARD, San Diego, CA).

The machine was calibrated before each round of mice to ensure that the temperature gradually increased at a rate of one degree per second to activate heat-sensitive C-fibers (Yeomans, Proudfit, 1996). Temperatures at 0, 5, 10, 15, and 20 seconds were recorded. Calibration was performed for each set of mice prior to acclimation period, at a minimum of three times per testing day. The calibration curve derived was a linear function showing the relationship

between time and temperature of the Hargreaves apparatus. Plotted temperature was the average of the temperature of the three calibration periods.

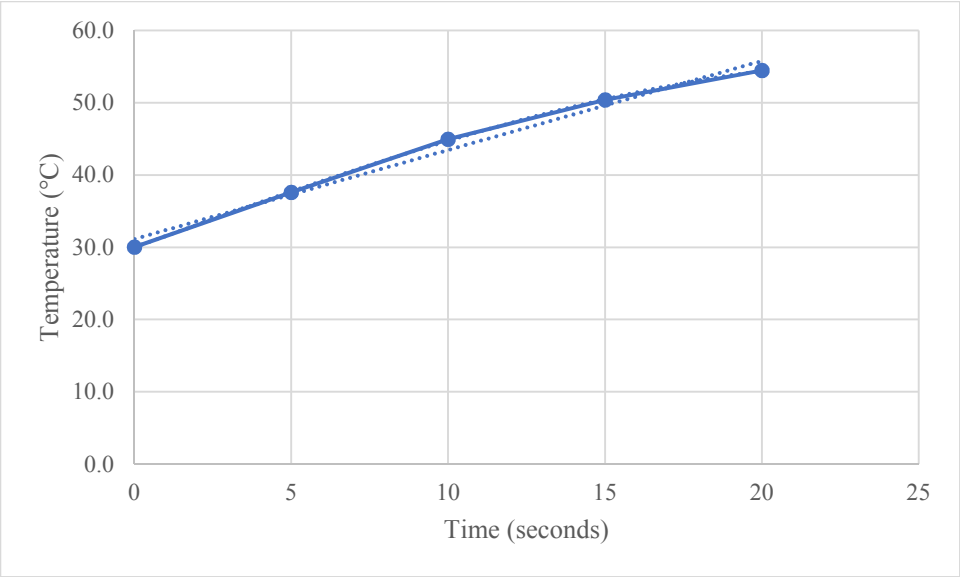

Figure 1. Linear calibration curve for thermal nociception test. Time and temperature have a directly proportional relationship. The polynomial equation depicting the relationship between time and temperature is $y = -0.0008x^3 – 0.0028x^2 + 1.5775x + 30.002$.

Mice were placed atop the glass sheet of the thermal box that separated their paws from the heat source. Glass beakers were used as restraint chambers. Mice were acclimated to the thermal box fifteen minutes prior to the test. During acclimation, the testing apparatus was warmed to 30°C.

During testing, the heat source was placed underneath the plantar region of the paw and gradually increased temperature over time. The temperature at which mice produced a paw withdrawal response (licking the paw, flinching, or raising the paw) was monitored and recorded for four repetitions of the test. Both hindpaws of each animal were tested. The median temperature of the last three trials was used in statistical analysis. If an animal urinated at any point during testing, urination was wiped from the animal's hindpaws, from the glass beaker, and the glass sheet to avoid issues with heat transfer.

b. Rotorod Testing

To test sensorimotor coordination to ensure that the diseased mice can perform paw withdrawal response-based tests and do not have impaired coordination, rotorod testing was performed in conjunction to thermal response testing and von Frey filament testing, using the Rotarod machine (Rotarod, Stoelting Co.). For mice, rotating rods were 1.25

inches in diameter. Mice were placed on an increasingly rapidly rotating rod and were monitored on how long they could keep their balance on the rotating rod. Prior to the test, the animals performed a test run to acclimate to the rotating rods. Plates underneath the mice that sensed the weight of the mice stopped the test when all animals fell from the rod. The rate, time, and distance at which they ran were recorded.

Histological Analyses

Tissue collection of eyes, foot skin, sciatic nerve, and DRGs was performed at the end of eight weeks. For analysis of corneal images, axonal caliber, and foot skins, animal tissues were coded and randomized to perform double-blinded analysis.

I. Corneal confocal microscopy

Corneal confocal microscopy was used to analyze nerve structure and quantify nerve density in the cornea. The two layers of the cornea that were analyzed were the sub-basal nerve plexus (SBNP) and the stroma layer. Confocal microscopy was performed by using the Heidelberg Retina Tomograph 3 (HRT 3 with Rostock Cornea Module) and Heidelberg Eye Explorer (Heidelberg Engineering Inc., Franklin, MA, USA). Animals were anesthetized in an induction chamber at 2.5 ppm with isoflurane and monitored for breathing. While under anesthesia, animals were strapped upon a platform with an isoflurane breathing mask and positioned to expose an eye to the laser. Lubricant eye gel was applied to exposed eyes to prevent dryness. The laser was positioned at the middle of the cornea of each mouse and the depth was repositioned to start at the beginning of the SBNP layer. Upon positioning the laser, the laser camera captured volumetric sets of images from the SBNP layer into the stromal layer. Both eyes of each animal were captured by the machine and subsequently analyzed.

Analysis of corneal images was performed using program ImageJ (Image Processing Analysis in Java, National Institutes of Health). Five images of the SBNP layer and ten images of the stromal layer were analyzed. With Image J software, nerves in each image were traced using a tracing pad and an electronic pen. Visible nerves that were traced were bright white lines against a black and gray background (Fig. 2). Bright white cell bodies, wrinkles, scars, and signs of infection (white blotches against a black and gray background) were not counted. Nerve density of corneal images were quantified in number of pixels.

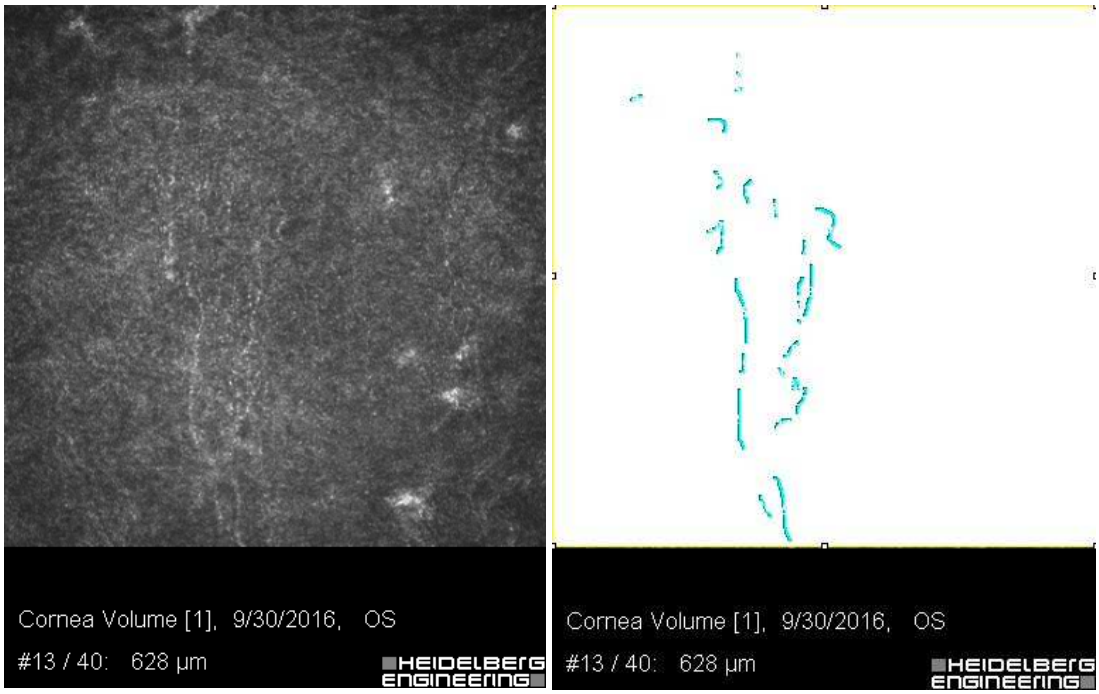

Figure 2. (a) Corneal confocal microscopy image in the sub-basal nerve plexus (SBNP) layer. Nerves are thin, white lines against dark background. Note lack of white cell bodies in the SBNP layer. **(b)** Nerve density quantification in pixels. Nerves were traced using ImageJ software.

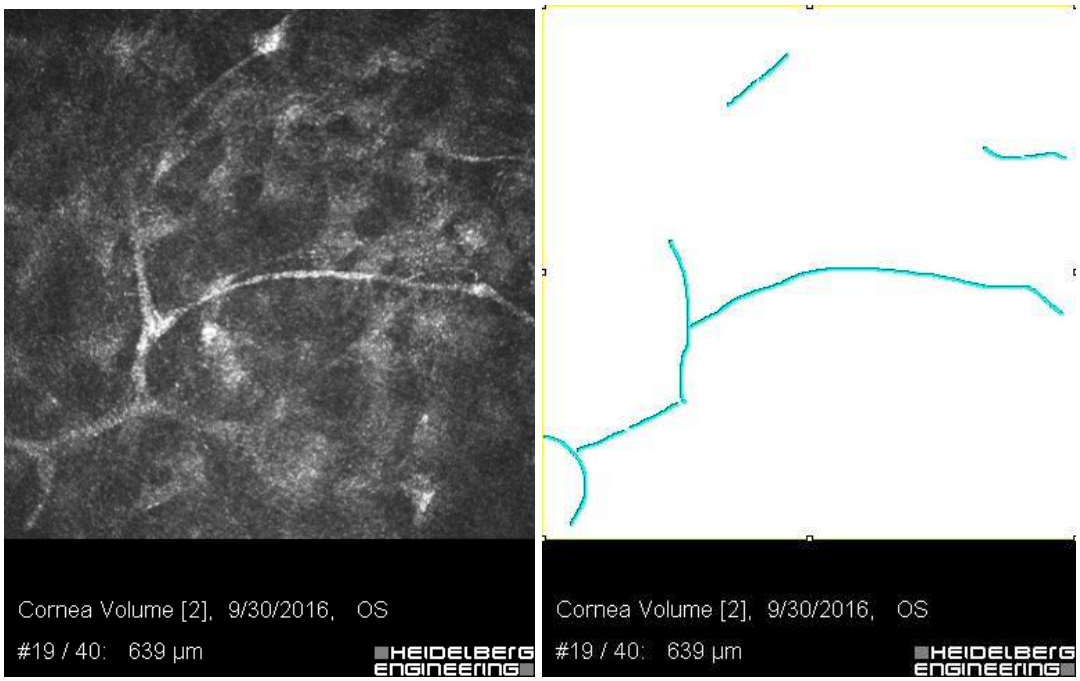

Figure 3. (a) Corneal confocal microscopy image in the stromal layer. Nerves are thick, white lines against dark background. Note presence of white cell bodies in the stroma layer. **(b)** Nerve density quantification using ImageJ software. Nerves were traced and quantified in pixels.

II. Foot skin microscopy

Plantar skin was collected from both the left and right paw of each mouse. Each piece of tissue was laid flat upon perforated pieces of plastic to allow for greater exposure of tissues to fixatives. Upon placing tissues on the plastic, each tissue was placed in scintillation vials of 10 mL of 4% buffered paraformaldehyde and were fixed overnight at 4°C.

The following day, tissues were rinsed three times with 10 to 20 mL of 0.1 M sodium phosphate buffer (1:1 dilution of water to 0.2 M sodium phosphate buffer). During each round of rinsing, tissues were swirled around in scintillation vials. After rinsing, tissues were stored in 0.1 M sodium phosphate buffer at 4°C.

Embedding of foot skins required the following materials: an embedding cassette, a lead pencil, forceps, paraffin and a paraffin processor. Mice foot skins were embedded in blocks of 4% paraffin. Blocks were cut in sections of six micrometers using a rotary microtome and two sections of six micrometers were placed onto slides which were stained using PGP9.5. Both sections of each slide were analyzed for overall staining consistency and structure of the foot skins. Foot skins that included numerous oil glands, hair, tears in the dermis, overlapping sections or indentations

would be considered foot skins of lower quality and would be less likely to be considered a candidate for analysis. One foot skin was chosen for each slide to be counted and was marked with an arrow.

Analysis and quantification of nerves in the foot skin were performed under 40x magnification using a light microscope. Intraepidermal nerve fibers (IENFs) and subepidermal nerve plexus (SNP) fibers were quantified for each foot skin sample. Parts of the foot skin that included oil glands, hair, tears, or indentations were skipped and noted in sketches of the foot skin.

The length of the foot skin was calculated using a light microscope under 20x magnification, ScionImage software, and a tracing pad with an electronic pen. Using the length in millimeters calculated with ScionImage, the nerve density was calculated:

$$IENF\ nerve\ density\ \left(\frac{nerves}{mm}\right) = \frac{\#\ of\ IENF\ counted}{length\ of\ nerve}$$

$$SNP\ nerve\ density\ \left(\frac{nerves}{mm}\right) = \frac{\#\ of\ SNP\ counted}{length\ of\ nerve}$$

III. Axonal caliber and myelin sheath area analysis

To visualize and measure large motor and sensory nerve fibers, the left sciatic nerve was first fixed in resin blocks using 2.5% glutaraldehyde. Resin blocks of sciatic nerve were cut using a microtome to sections that were 6um thick. Sections were placed onto glass slides and stained with *p*-Phenylenediamine (PPD). Of the sections, cross sections that were chosen did not have artifacts such as folds or tears and had most even staining.

Sciatic nerves were imaged using the program Image-Pro Premier and light microscopy at 60x magnification. Sciatic nerves were chosen were free of artifacts such as distortions, stretched axons, crushed axons.

Axonal caliber was measured using ScionImage and myelin sheath area and g-ratio were measured using an in-lab created program named MarvoQuant (Adobe Photoshop 4, Adobe Inc., California, USA). Nerve cross sections that were counted in the program had intact myelin sheaths and were circular or oval in shape. The nerves should not have any artifacts such as tears or Schwann cell nuclei or appear stretched, crushed, or distorted in any fashion. To calculate the g-ratio, the following calculation was used:

$$g - ratio = \frac{diameter\ of\ axon\ (d)}{diameter\ of\ myelinated\ axon\ (D)}$$

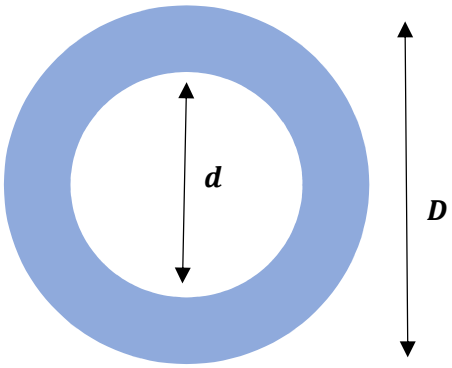

Figure 4. Graphic depiction of a myelinated axon. D = diameter of whole myelinated axon; d = diameter of axon only.

IV. Statistical analysis

All statistical analyses used one-way ANOVA with Dunnett's test and were calculated using Graphpad Prism v7 technology. Graphs were made using Excel or GraphPad Prism v7 technology.

RESULTS

Barbering and Fighting Behaviors

Prion disease mice showed extensive barbering behavior, leading to baldness, dermatitis, and in one case, severe injury of the left flank. This behavior may have affected results of behavioral testing such as thermal nociception testing, von Frey filament testing, rotorod testing, and MNCV testing. Thermal testing, von Frey filament testing, and rotorod testing depend upon pain responses and motor coordination, which could have been affected by pain from barbering. MNCV data for the mouse with severe injury of the left flank may have also been affected by potential damage to the sciatic nerve. Male control mice also showed fighting behavior that resulted in scarring of the cornea, which could have affected the quantification of corneal nerves. Any animals with severe barbering or fighting behaviors were placed in separate cages to minimize further injuries to themselves and other cage mates.

General Health

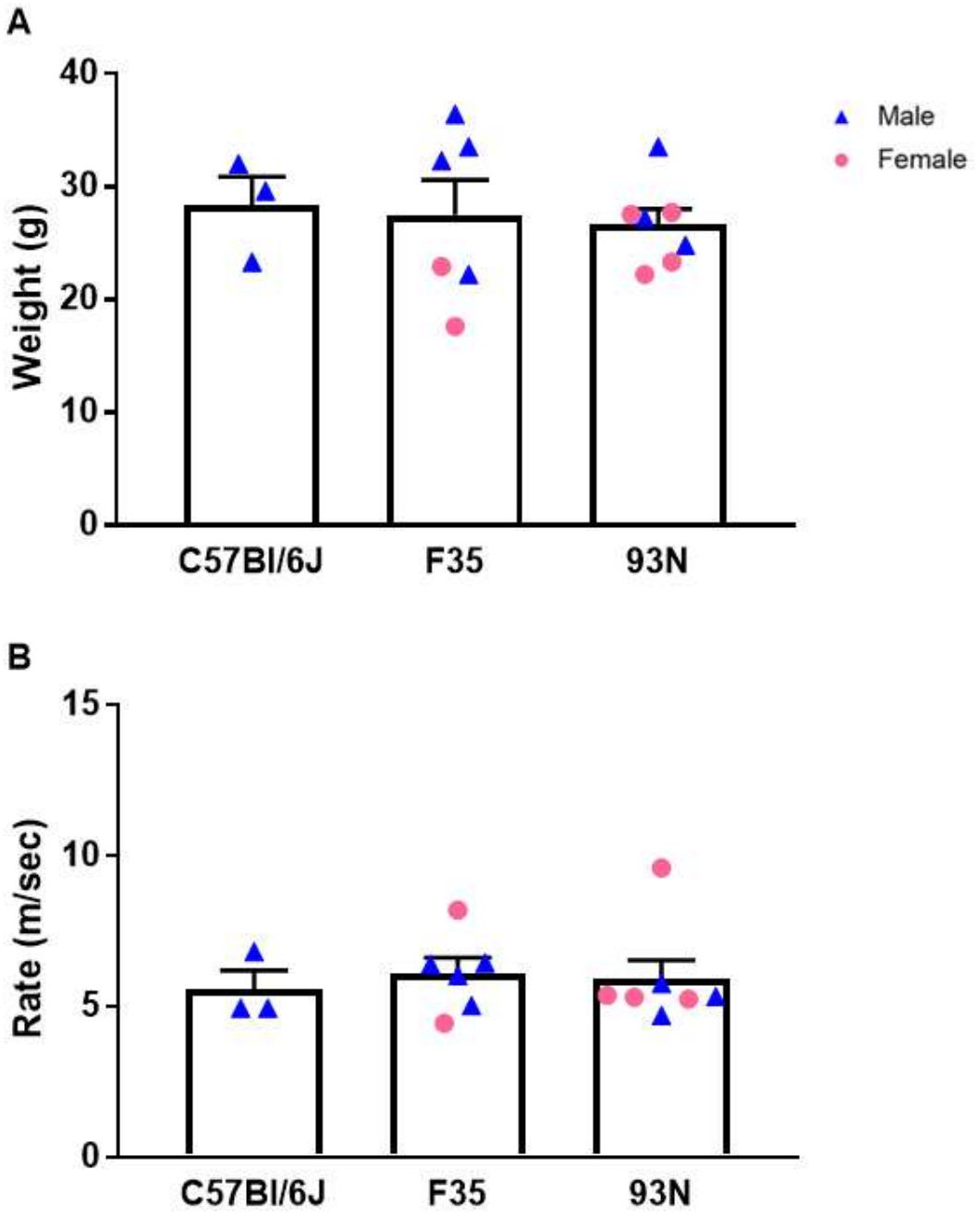

Figure 5. (A) Terminal body weight and **(B)** rotorod testing of general sensorimotor function. All data are mean + SEM. Control animals are C57Bl/6J mice (N=3), and experimental groups are F35 (N=6) and 93N (N=7). Statistical comparisons of prion mice models C57Bl/6 mice (N=3), and experimental groups are F35 (N=6) and 93N (N=7). Statistical comparisons of prion mice models C57Bl/6J to F35 and C57Bl/6J to 93N were performed by ordinary one-way ANOVA with post-hoc Dunnett test ($p>0.05$).

All mice were weighed to assess overall health (Fig. 5A). In comparing terminal body weights of the two prion mouse models to that of the control group, both F35 (27.5 + 3.1 g) and 93N (26.6 + 1.4 g) mice weights were comparable to that of control mice (28.3 + 4.5 g).

To assess if prion mice had enough sensorimotor coordination to participate in behavioral testing, rotorod behavioral testing was performed (Fig. 5B). F35 mice and 93N mice show sensorimotor skills comparable to that of controls. Both prion disease mouse model groups show similar rates (F35 mean + SEM = 6.1 + 0.5 m/sec, 93N mean + SEM = 5.9 + 0.6 m/sec) to control mice (C57Bl/6J mean + SEM = 5.6 + 0.6 m/sec). While prion disease mice still had behavioral characteristics such as tremors and ataxia, results of rotarod testing illustrates that F35 mice and 93N mice did not show deficits in sensorimotor function that would inhibit other behavioral tests. Because no differences in sensorimotor function among the groups were found, behavioral tests such as thermal testing and tactile testing, which involve paw withdrawal responses, will not be obfuscated by the prion mice's abilities to withdraw their paws and that they are still healthy enough to participate in the behavioral tests. Any deficits found in behavioral tests can then be attributed to peripheral neuropathy, not to impaired sensorimotor coordination in disease models.

Small Fiber Function

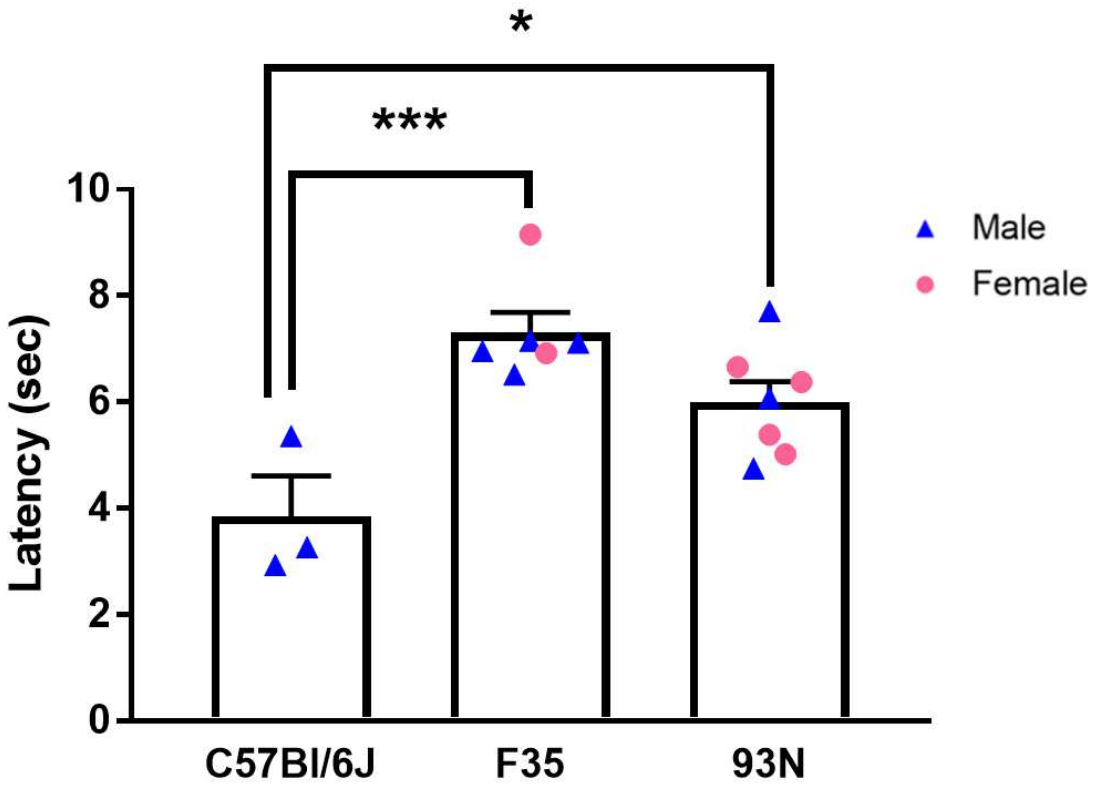

Figure 6. Latency of paw withdrawal response to thermal stimuli. Data are mean + SEM. Control group are C57Bl/6J (N=3). Experimental groups are F35 mice (N=6) and 93N mice (N=7). Statistical comparison of C57Bl/6J to F35 and C57Bl/6J to 93N was performed by ordinary one-way ANOVA test with post-hoc Dunnett test (*= $p<0.05$; ***= $p<0.001$). Statistical comparison between male and female mice within F35 and 93N groups were performed by unpaired student t-tests ($p>0.05$).

Both F35 (7.30 + 0.38 sec) and 93N (6.00 + 0.39 sec) mice showed significantly ($p<0.05$ and $p<0.001$, respectively) longer paw withdrawal latencies in response to thermal stimuli, compared to control mice (3.85 + 0.76 sec). While F35 mice showed slightly higher latencies than that of 93N mice, the response latencies of both groups were comparable to one another.

Male and female mice within groups F35 and 93N did not show differences in paw withdrawal latencies. In the F35 group, female F35 (40.92 + 1.48 sec) and male F35 mice (39.66 + 0.23 sec) had similar paw withdrawal latencies. Likewise, in the 93N group, female 93N (38.49 + 0.47 sec) and male 93N mice (39.39 + 0.84 sec) showed comparable paw withdrawal latencies.

Small Fiber Structure

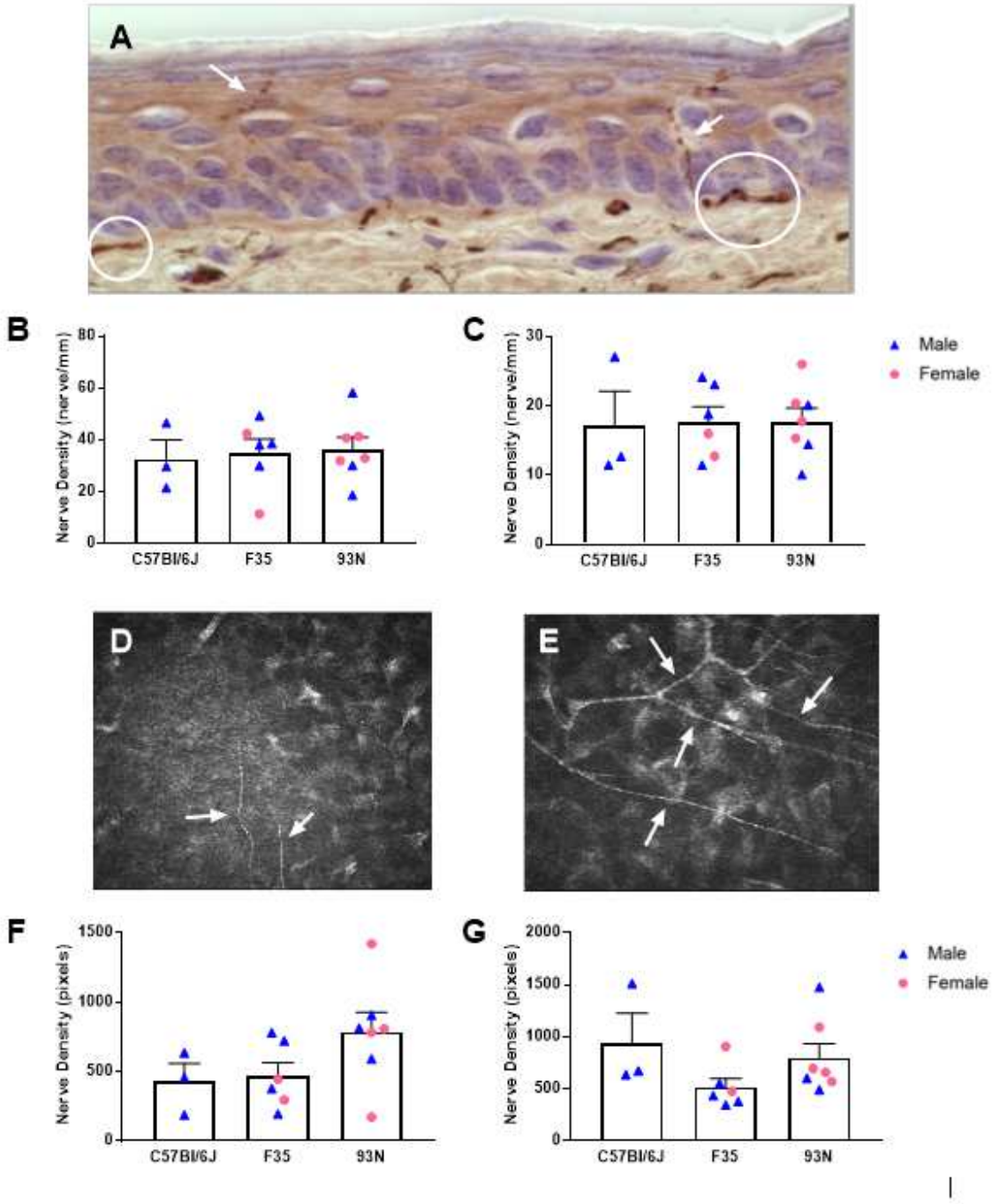

Figure 7. Small fiber density in left mouse foot skin and mouse eyes**. (A)** Light micrograph of mouse foot skin. Profiles of intraepidermal nerve fibers (IENF: arrows) and sub-epidermal nerve plexus (SNP: circled). **(B)** SNP and **(C)** IENF density per millimeter length of mouse foot skin. **(D)** Confocal micrograph of sub-basal nerve plexus (SBNP) and **(E)** stromal layer of mouse cornea. Profiles of SBNP and stromal nerves are denoted with white arrows. **(F)** SBNP and **(G)** stromal nerve fiber density of mouse eye, in pixels. All data are mean + SEM. Statistical comparison of F35 (N=6) and 93N (N=7) groups against C57Bl/6J (N=3) was performed by

(Figure 7. Continued) ordinary one-way ANOVA with post-hoc Dunnett test ($p>0.05$). Statistical comparison of male and female mice within F35 and 93N groups performed by multiple unpaired student t-tests ($p>0.05$).

To analyze the connection between small sensory nerve function and small fiber structure and nerve density in the paw, sensory nerves were also quantified in paw skin (Fig. 7A and 7B). Foot skin nerve densities of sub-epidermal nerve plexus (SNP) and intraepidermal nerve fibers (IENF) showed no significant differences between the control group and both prion disease models. Both F35 mice SNP nerve density (34.94 + 5.37 nerves/mm) and IENF nerve density (17.70 + 2.15 nerves/mm) were virtually the same as that of the C57Bl/6J mice (SNP density = 32.59 + 12.77 nerves/mm; IENF density = 17.07 + 5.00 nerves/mm). 93N mice showed similar SNP and IENF nerve density counts to both F35 mice and control mice, as well (93N SNP density = 36.28 + 4.65 nerves/mm; 93N IENF density = 17.72 + 1.93 nerves/mm.

To determine whether retention of sensory nerve densities was systemic, sensory nerves were also quantified in the cornea (Fig. 7C and 7D). As with sensory nerve density in foot skins, 93N mice and F35 mice showed no significant differences in corneal nerve density of nerves in either the sub-basal nerve plexus or stromal layers compared to controls. 93N mice had a mean nerve density in the SBNP of 784.14 pixels + 140.95 pixels compared to that of F35 mice (468.30 pixels + 95.62 pixels) and C57Bl/6J control mice (392.07 pixels + 123.77 pixels). In the stroma, 93N mice had a mean nerve density of 797.74 pixels + 134.55 pixels compared to F35 mice stromal nerve density of 515.22 pixels + 83.78 pixels. Both F35 mice and 93N mice had lower trends of stromal nerve density compared to control mice (939.43 pixels + 285.82 pixels) (Fig. 7D).

Lack of significant deficits in both SBNP and stromal nerve densities between the prion disease mouse models and the control group indicates an absence of significant structural abnormalities in small sensory nerves of F35 and 93N mice, despite significant deficits in comparable peripheral sensory nerve functions such thermal nociception (Fig. 6). To explore if large motor nerve fiber function was affected in both prion disease mouse models, we performed von Frey filament testing and motor nerve conduction velocity (MNCV) testing.

Large Fiber Function

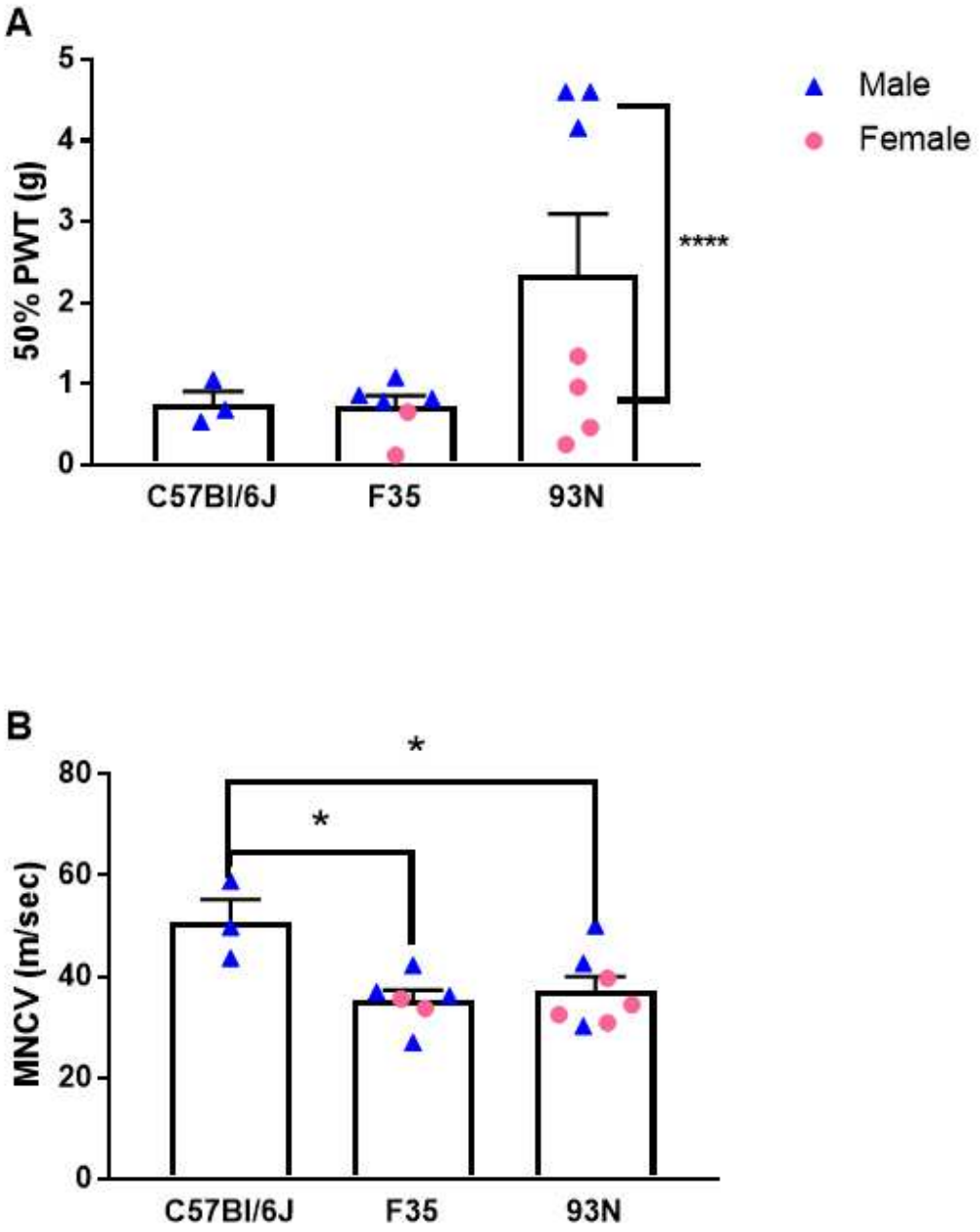

Figure 8. (A) Measurement of paw withdrawal response to tactile stimuli. 50% PWT is the paw withdrawal threshold, after which the mice withdraw their paws from the tactile stimuli 50% of the time (measured in grams). Data are mean + SEM. Control animals are C57Bl/6J mice (N=3). Experimental groups were F35 mice (N=6) and 93N mice (N=7). Statistical comparison of C57Bl/6J to F35 and C57Bl/6J to 93N was performed by ordinary one-way ANOVA with post-hoc Dunnett test ($p>0.05$). Statistical comparisons of male to female in F35 and 93N groups were performed by multiple unpaired student t-tests. ****=$p<0.0001$. **(B)** Motor nerve conduction velocity (MNCV) measurements of left flank, measured in m/sec. Data are mean + SEM. Control animals are C57Bl/6J mice (N=3). Experimental groups were F35 mice (N=6) and 93N mice (N=7). Statistical comparisons of male to female in F35 and 93N groups were performed by multiple unpaired student t-tests ($p>0.05$). Statistical comparison of F35 mice and 93N mice to controls was performed by ordinary one-way ANOVA with post-hoc Dunnett test. *= $p<0.05$.

Von Frey filament testing was performed to measure sensitivity to mechanical stimuli. Compared to the control C57Bl/6J group (0.30 + 0.13 g), F35 mice did not show significant difference in paw withdrawal threshold (0.25 + 0.13 g). As a whole, the 93N group was also comparable to controls (0.65 + 0.22 g). 93N females did not show any significant difference in paw withdrawal threshold (0.92 + 0.25 g) compared to the control group. However, 93N males showed a significantly ($p<0.0001$) higher paw withdrawal threshold compared to 93N females indicating sexual dimorphism in paw withdrawal response to tactile stimuli. Sexual dimorphic patterns were absent in the F35 group.

While large fiber responses to mechanical stimuli were similar among prion disease mouse models and control groups, both F35 mice and 93N mice showed significant ($p<0.05$, $p<0.05$) slowing of motor nerve conduction velocity (MNCV) compared to the control group. While control mice had a mean MNCV of 50.8 + 4.4 m/sec, F35 mice and 93N mice had mean MNCVs of 35.3 +7.0 m/sec and 37.2 + 2.8 m/sec, respectively. Both prion disease mouse models showed similar MNCV measurements. Sexual dimorphic patterns were absent in both F35 and 93N groups.

To explore a structural correlate to large fiber MNCV slowing noted in both mouse models of prion disease (Fig. 8B), we measured axonal of large myelinated nerve fibers in the sciatic nerve.

Figure 9. (A-C) Light micrographs of control, F35, and 93N mouse sciatic nerves, respectively, at 60x. A=axon. Note differences in thickness of myelination between control mice and prion disease mice. **(D)** Axonal size-frequency distribution, **(E)** mean axon diameter (MAD) density, **(F)** mean axonal density of large nerve fibers, **(G)** and g-ratio in mice sciatic nerves**,** with corresponding inset graphs of male mice in each group**.** All data are mean + SEM. Control mice are C57Bl/6J mice (N=3). Statistical comparison of F35 mice (N=6) and 93N mice (N=7) against C57Bl/6J controls was performed by ordinary one-way ANOVA with post-hoc Dunnett test (*= $p<0.05$; **= $p<0.01$; ***= $p<0.001$; **** = $p<0.0001$). Statistical comparison between male and female mice within F35 and 93N groups was performed by multiple unpaired student t-tests. ($p>0.05$).

Figure 9. Continued. (A-D)

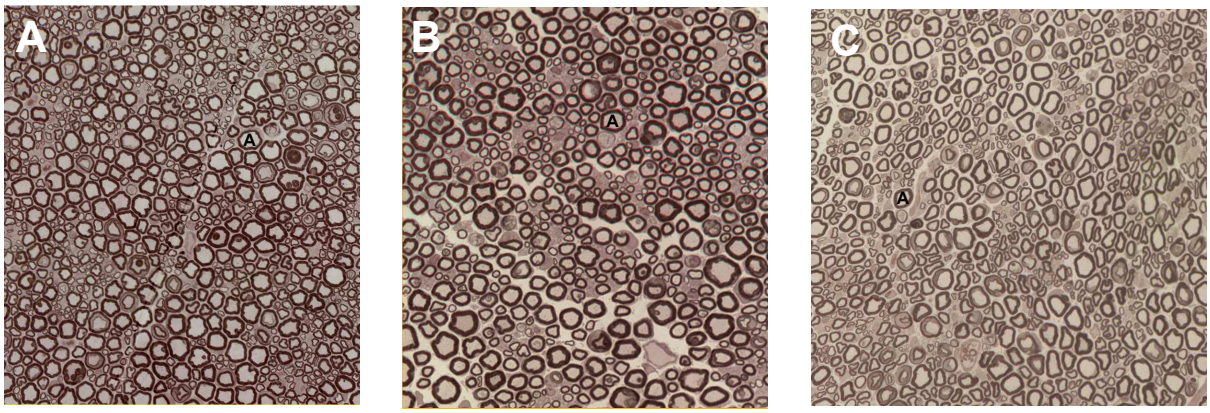

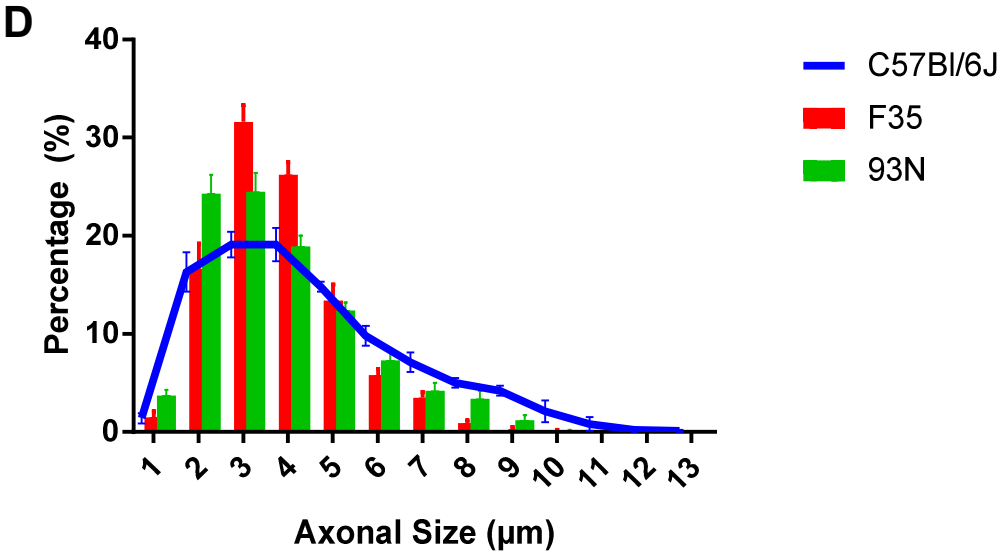

Figure 9. Continued. (E-G)

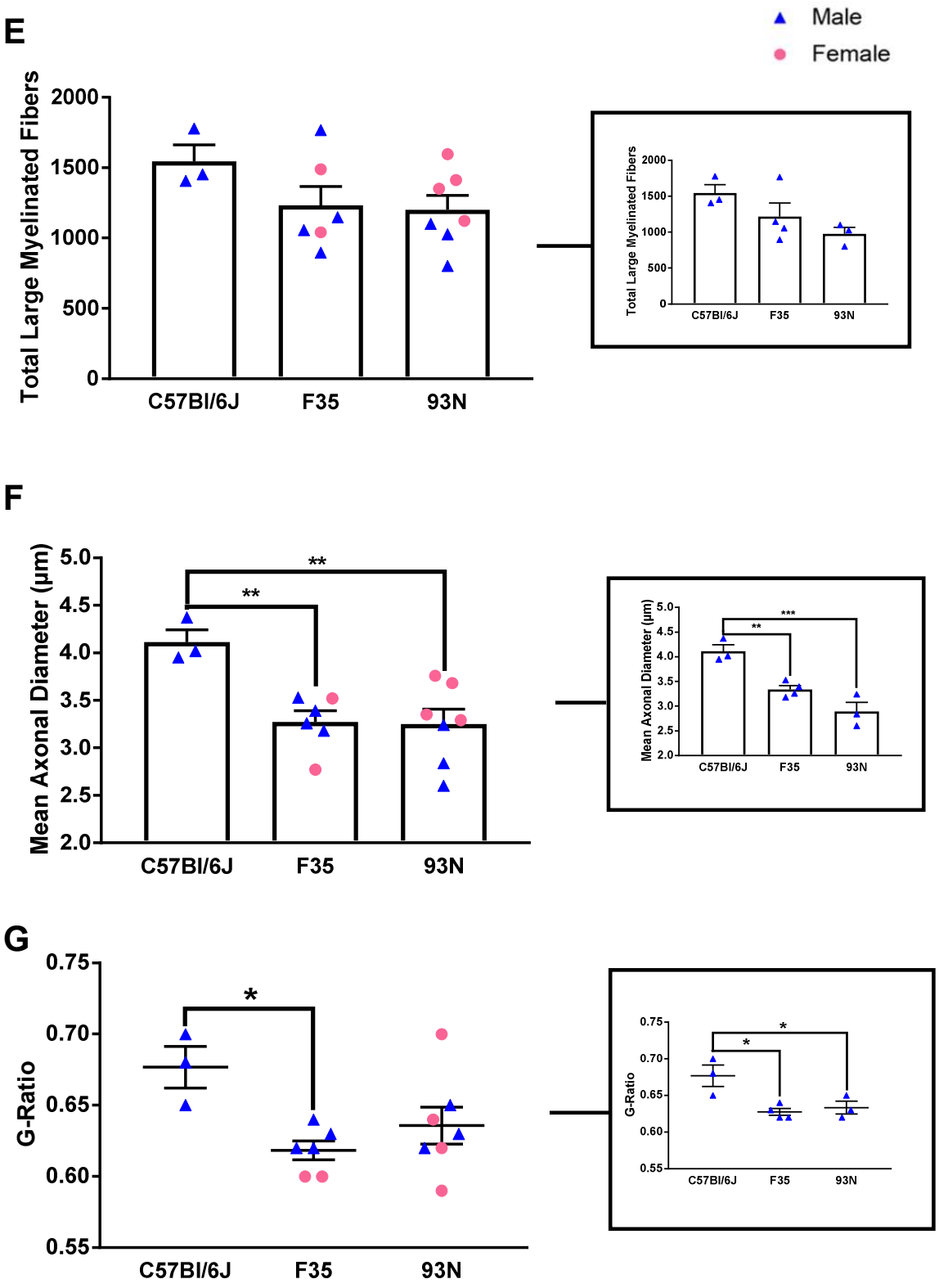

Large Fiber Structure

Axonal size was grouped into three descriptive size categories: “small fibers” to denote axonal calibers between 1 μm and 5 μm; “medium fibers” to denote axonal calibers between 6 μm and 12 μm; and “large fibers” to denote axonal calibers between 13 μm and 20 μm (Fig. 9D). Overall, the axonal size-frequency distribution of all groups was heavily skewed toward small axon calibers, peaking at axonal diameter of 3 μm. No groups had axonal calibers above 13 μm in diameter.

Of the small fibers, both F35 mice (31.6 + 1.7 axons) and 93N mice (24.5 + 1.9 axons) showed significantly higher frequencies of 3 μm axons compared to that of control mice (19.1 + 1.3 axons) ($p<0.0001$, $p<0.01$, respectively). 93N mice (24.3 + 1.9 axons) also showed a significantly higher frequency ($p<0.0001$) of 2 μm axons compared to that of control mice (16.3 + 2.0 axons). While F35 mice showed no significant differences in the frequency of 2 μm axons compared to control mice, F35 mice (26.2 + 1.3 axons) did show a significantly higher frequency ($p<0.001$) of 4 μm axons than did control mice (19.1 + 1.7 axons). Prion disease mice showed no significant differences compared to control mice in their frequencies of axonal calibers of 1 μm and 5 μm.

Overall, both F35 mice (1232.3 + 134.3 axons) and 93N mice (1144.4 + 145.2 axons) showed no significant deficits in mean axonal density of large myelinated fibers within their sciatic nerves compared to control mice (1545.7 + 117.5 axons) (Fig. 9E). However, both prion disease mouse models also showed significantly reduced mean axonal diameter (F35 = 3.3 + 0.1 μm, $p<0.01$; 93N = 3.3 + 0.2 μm, $p<0.01$) compared to control mice (4.1 + 0.1 μm) (Fig. 9F).

To analyze myelination of prion disease mice compared to that of control mice, g-ratio analysis was performed (Fig. 9G). Only the F35 group (0.62 + 0.01) showed significantly lower g-ratio ($p<0.05$) than control mice (0.67 + 0.01) upon first analysis. 93N mice (0.64 + 0.01) showed a mean g-ratio comparable to that of control mice.

Because sexual dimorphism of peripheral neuropathic phenotypes was seen in von Frey filament testing results of 93N male mice, post-hoc statistical analysis of all male mice was performed on mean axonal diameter data, large myelinated fiber data, and g-ratio data. While there were no significant differences in the total number of large myelinated fibers between the prion disease mice models (F35 = 1216. 0 + 190.9 axons, 93N = 976.7 + 89.9 axons) and control mice (1545.7 + 117.5 axons) (Fig. 9E insert), the mean axonal diameters of both 93N males (2.9 + 0.2 μm, $p<0.001$) and F35 males (3.3 + 0.1 μm, $p<0.01$) were significantly smaller than that of control mice (4.1 + 0.1

μm) (Fig. 9F inset). G-ratio post-hoc analysis comparing all male mice among each group showed both F35 males (0.63 + 0.01, $p<0.05$) and 93N males (0.63 + 0.01, $p<0.05$) had significantly lower G-ratios compared to control males (0.67 + 0.01) (Fig. 9G inset).

DISCUSSION

Peripheral Neuropathy in Prion Disease

Spongiform encephalopathy and attendant CNS dysfunction have long been the major focus of investigations of prion diseases. However, sciatic nerves of CJD patients and transgenic prion mouse models show deposits of mutant prion proteins, and it is now well recognized that peripheral nerves are established routes of neuroinvasion and mutant protein propagation (Crozet et al., 2007; Favereaux et al., 2004; Aguzzi et al., 2003).

Peripheral neuropathy in patients with prion disease affects both sensory and motor nerves. A recent autopsy study reported that 50% of a group of patients with sporadic or familial prion disease had axonal polyneuropathy or demyelinating polyneuropathy that correlated to antemortem reports of loss of sensation in hands and feet (Wang et al., 2018). In studies of patients with CJD caused by E200K mutation, nearly all patients showed some form of peripheral neuropathology such as motor neuron disease, axonal-demyelinating neuropathy and axonal disease, despite lack of peripheral neuropathic symptoms (Neufield et al., 1992; Niewiadomska et al., 2002).

Peripheral neuropathy in herd animals has not been studied extensively, but studies report that prion protein deposition occurs in peripheral nerves of BSE-affected cattle (Okada et al., 2012). Transgenic mouse models of prion disease also exhibit prion protein deposition in peripheral nerves (Crozet et al., 2007). Experimental models of peripheral neuropathy in prion disease show that mice with complete ablation of both Prnp alleles are prone to developing peripheral neuropathy. Conversely, transgenic mouse models of prion disease that overexpress wild-type prion protein also exhibit demyelinating neuropathy (Westaway et al., 1994). Despite these findings, little else is known of peripheral neuropathy in experimental models of prion disease.

Our Models of Prion Disease

The F35 knock-out mouse model has a deletion of residues Δ32-134 within the N-terminus of the host-encoded prion protein. Transgenic F35 knock-out mice are one of many common mouse models of prion diseases in which segments of residues within the N-terminus are deleted to discover their function within the prion protein

(Fischer et al., 1996; Shmerling et al., 1998; Li et al., 2007). While studies have documented neurodegenerative symptoms in the central nervous system such as cerebellar ataxia, no studies have documented peripheral neuropathy in transgenic F35 mice.

The 93N mouse model has a point substitution modification on the N-terminus and can aid in discovering the function of each domain of the native prion protein and its neurotoxic pathway. Ongoing research has shown normal CNS development of prion mouse models with modified C-terminals that contrasts with marked encephalopathy in mice with modified N-terminuses, either by deletion of part of the N-terminus or a substitution mutation (Sigurdson Lab, Personal Communication, unpublished data). These results further support the hypothesis that N-terminus of the prion protein is the neurotoxic domain of the prion protein (Wu et al., 2017; Yoshikawa et al., 2008). No known peripheral neuropathic symptoms have been characterized in 93N mice prior to this thesis.

Large Fiber Motor Neuropathy

Measuring motor nerve conduction velocity (MNCV) of large motor fibers in the sciatic nerve is a standard procedure in studies of peripheral neuropathy. Impairment of MNCV was seen in both F35 and 93N mice and in both sexes within each model. Large fiber conduction velocity is conventionally considered to be determined by axonal diameter, myelin thickness and intermodal distance (Waxman, 1980) although the membrane biophysics of action potential propagation at the node of Ranvier can also contribute in the absence of structural pathology (Wu et al., 2012). To determine whether impaired MNCV was associated with structural pathology, we quantified the total number of large nerve fibers, mean axonal diameter and axonal size-frequency distribution in the sciatic nerve. There was no statistically significant difference in the number of large nerve fibers per sciatic nerve, indicating that there was not selective fiber loss. However, both prion disease models showed significantly smaller mean axonal diameters than control mice and axonal-size frequency distributions were skewed toward much smaller axonal calibers. In the absence of fiber loss, this shift could reflect either impaired maturation of fibers or atrophy of mature fibers. Measurements of axonal diameter at earlier time points would allow discrimination of these two possibilities.

To explore if our experimental prion disease models had undergone axonal shrinkage, we calculated the g-ratio of axons in the sciatic nerve. The g-ratio represents the ratio between the diameter of an axon and the diameter of the entire myelinated fiber (axon+myelin). The optimal g-ratio for maximum nerve conduction velocity is

approximately 0.60 in the peripheral nervous system (Chomiak and Hu, 2009). G-ratios that vary from 0.60 are associated with neurodegenerative disease (Fields, 2008). In the case of impaired maturation of fibers, one would predict axonal shrinkage with compensatory myelin thickening to preserve an optimal g-ratio of 0.6. However, g-ratio calculations showed that F35 mice had lower g-ratio values than control mice, while 93N mice showed comparable g-ratio values to control mice. Upon exploratory post-hoc analysis of only male mice, both F35 and 93N male mice showed significantly lower g-ratio values compared to those of control mice. Lower g-ratios can be attributed to thickening of the myelin sheath or shrinkage of axonal diameter without concurrent thinning of myelin. As mean axonal diameter is significantly smaller in F35 and 93N mice than in control mice, shrinkage of axonal diameter without myelin thinning appears to be more likely than thickening of the myelin sheath. The axon caliber size-frequency distribution also supports the potential for axonal shrinkage, as both F35 and 93N axon-caliber size-frequency curves are skewed toward smaller axonal calibers. Axonal atrophy with concurrent slowing of MNCV has been reported in rat and mouse models of diabetic neuropathy (Anders et al., 1983; Yagihashi et al., 1999; Zochodne et al., 2004). Recall that axonal neuropathy has also been reported in patients with CJD alongside demyelinating polyneuropathy (Neufield et al., 1992). To confirm that lower g-ratios are due to axonal shrinkage and not due to thickening myelin sheaths, mean area of myelin sheaths should be quantified.

It is notable that most studies document demyelinating polyneuropathy as the prevailing form of peripheral neuropathy in prion disease patients and mouse models (Westaway et al., 1994; Niewiadomska et al., 2002). Native prion protein regulates axonal myelination and its ablation leads to symptoms of chronic demyelinating polyneuropathy (Bremer et al., 2010). Alterations and mutations of the native protein may therefore disrupt myelination. Levels of myelin basic protein in the central nervous system are severely decreased in 93N mice compared to wild-type mice, supporting the idea that myelination is affected (Dr. Sigurdson's Lab, Personal Communication, unpublished data). As the mutant prion invades the central nervous system via the peripheral nervous system (Glatzel et al., 2004), future experiments should investigate levels of myelin basic protein in the PNS. Additionally, as Schwann cells communicate with axons during axonal injury to perform myelination, further research should investigate for potential Schwann cell pathologies in the sciatic nerve (Taveggia, 2016).

Large Fiber Sensory Dysfunction & Sexual Dimorphism

To determine if large sensory fiber dysfunction may occur in conjunction with MNCV slowing and axonal shrinkage, I performed von Frey filament testing on the F35 and 93N mice. von Frey filament testing specifically assesses large sensory fiber function via behavioral nocifensive responses to mechanical stimuli by quantifying the paw withdrawal response threshold (Chaplan et al. 1994; Deuis et al., 2017). von Frey filament testing can identify the presence of increased sensitivity to normally non-noxious pressures (tactile allodynia) or loss of sensitivity to normally noxious stimuli (hypoalgesia). Results of von Frey filament testing indicated that F35 and 93N mice showed no significant deficits in large sensory nerve fiber function. However, after performing an exploratory post-hoc statistical analysis between female and male mice, 93N male mice showed significantly higher paw withdrawal thresholds compared to 93N female mice. This is indicative of hypoalgesia - decreased sensitivity to mechanical stimuli. This sexual dimorphism in large sensory fiber dysfunction was specific to the 93N group. Tissue-specific sexual dimorphism has been observed in other neurodegenerative diseases. In clinical studies of Alzheimer's disease, affected men and women showed neurodegeneration in different areas of the hippocampus (Martinez-Pinilla et al., 2016). Transgenic mouse models of Alzheimer's disease have also recently been shown to have brain region- and sex-specific mitochondrial dysfunction (Djordjevic et al., 2017).

Reduced mean axonal diameter and the skewed distribution of axonal caliber towards smaller fibers in F35 and 93N mice may contribute to large fiber sensory dysfunction in 93N male mice. To confirm that reduced mean axonal diameter impacts large sensory fiber function, sensory NCV should also be determined. Potential slowing of sensory NCV could explain hypoalgesia as action potentials from afferent nerves may not be carried quickly enough to the spinal cord to produce a response to mechanical stimuli. However, it should be noted that reduced mean axonal diameter was observed in the sciatic nerve of both male and female F35 and 93N mice, whereas loss of mechanical sensation was restricted to male 93N mice. Sexual dimorphism in neuropathic symptoms has been reported in a clinical study, in which men have an earlier age of onset of neuropathic symptoms compared to female counterparts (Aaberg et al., 2008). As tactile hypoalgesia is associated with later stages of peripheral neuropathy, male mice with earlier onset of peripheral neuropathic symptoms may also experience late stage-associated symptoms much earlier than female counterparts.

No marked sensorimotor coordination deficits that would impact behavioral assays

We performed rotarod testing to assess sensorimotor coordination and determine whether prion mice were sufficiently coordinated to participate in behavioral assays during which they are required to lift their paws. Neither 93N nor F35 mice showed sensorimotor coordination deficits compared to control mice. This contrasts with a prior study that reported sensorimotor coordination deficits in *Prnp*-null mouse models of prion disease (Nazor et. al., 2007).

While cerebellar ataxia is a hallmark of prion disease in affected patients and some mouse models, even the smallest variation in mutations of the prion protein can lead to vastly different symptoms and disease progression of prion disease (Jackson et al., 2013). For example, two transgenic mouse models of Gerstmann-Straussler-Scheinker syndrome exhibited variations in prion disease presentation and progression Yang et al. (2009). Even homozygous null mouse models of prion disease are shown to have differences in pathology and disease progression (Weissmann and Flechsig, 2003). In our present study, the mutant prion protein in 93N mice is a result of a point mutation on the N-terminus of the native prion protein, while the truncated prion mutant in F35 mice is the result of a deletion at the N-terminus between amino acids 32 to 134. The absence of marked sensorimotor coordination deficits is thus consistent with the occurrence of unique behavioral phenotypes amongst different prion disease mouse models. Previous literature studying disease progression in homozygous transgenic F35 mice showed that prion disease in these mice reached its terminal stage around eighty-three days (Li et al., 2007). Neurodegenerative presentations such as cerebellar ataxia were reversed with over-expression of native prions. The age of our heterozygous F35 mice exceeded that of the animals in this study by forty days, yet our F35 mice still showed no marked deficits in coordination. This suggests rescue from severe disease via expression of a native prion allele in our heterozygous F35 mice. While disease progression of 93N mice has not been characterized, ongoing studies indicate that 93N mice maintain normal behavior and physiology but exhibit a steep decline in coordination and overall weight with age, with death at approximately five hundred days of age (Sigurdson Lab, Personal Communication, unpublished data). Our experimental 93N mice were much younger and thus were likely spared from more severe prion disease phenotype.

It is notable that we did not detect sensorimotor dysfunction in either the F35 or 93N mouse models of prion disease using the rotarod test. The rotarod test has been used in many mouse models of neurodegenerative

diseases to assess general sensorimotor coordination, including diabetic neuropathy, Alzheimer's disease, Parkinson's disease, and Huntington's disease (Jolivalt et al., 2016; Fleming et al., 2013; Taylor et al., 2011; Pallier et al., 2009). Models of neurodegenerative diseases with marked motor deficits, such as Parkinson's disease and Huntington's disease, show some sensorimotor impairment with rotarod testing, although results vary because rotarod testing may not measure subtle motor impairments (Fleming et al., 2013; Campos et al., 2013; Pallier et al., 2009). Predicted motor impairments of our prion disease mice are potentially similar to those of Parkinson's disease models, as cerebellar ataxia causes deficits in fine motor movement and gait, rather than impaired overall coordination. This notion is further supported by research in mice with cerebellar lesions, which show that subtle motor defects are not detectable by the rotarod assay (Stroobants et al., 2013). In models of peripheral neuropathy and neurodegenerative diseases, mice usually show no motor deficits (Chen et al., 2014; Schindowski et al., 2006).

Small fiber sensory dysfunction without change in small fiber structure

The Hargraves thermal nociception test has been widely used to assess function of small sensory nerve fibers via measuring sensitivity to noxious heat stimuli in animal models of peripheral neuropathy (Cheah et al., 2017; Hargreaves et al., 1988). The presence of thermal hyperalgesia is a common biomarker for early peripheral neuropathy and suggests inappropriate function of unmyelinated C-fibers (Kramer et al., 2004). Conversely, thermal hypoalgesia is a biomarker of late-term peripheral neuropathy and usually corresponds to decreased density of intraepidermal nerve fibers (IENF) that results in loss of sensation (Beiswenger et al., 2008). Animal models of neurodegenerative disease that experience denervation of foot skin as disease progresses include models of diabetic neuropathy (Beiswenger et al. 2008). I am not aware of any prior study that has measured paw thermal response latencies or IENF density in animal models of prion disease. However, there is accumulation and deposition of scrapie protein surrounding small nerve fibers in the foot skin prior to onset of clinical symptoms in transgenic hamster models of CJD, such as loss of sensation in the paws (Thomzig et al., 2007). We also used corneal confocal microscopy (CCM) to measure corneal nerve density in both the sub-basal nerve plexus and the stromal layers of the cornea (Chen et al., 2014). As the cornea is innervated by small C-fibers, utilizing CCM as a technique in identifying corneal denervation can aid in the diagnosis and early detection of small fiber peripheral neuropathy (Oliverira-Soto and Efron, 2001; Quattrini et. al., 2007; Papanas et al., 2013).

Both prion disease mouse models showed higher response latencies in response to thermal stimuli compared to control mice. Higher response latencies indicate decreased sensitivity to thermal stimuli, indicating the presence of thermal hypoalgesia. Despite small fiber sensory dysfunction, neither the foot skin nor the cornea of 93N and F35 mice showed deficits in small nerve fiber density compared to control mice. Prior descriptions of late onset peripheral neuropathy in five different knock-out strains and knock-in models of prion disease did not quantify small fiber (Wulf et al., 2017). This impairment of sensory function without change in small fiber structure indicates a dissociation between small nerve fiber function and nerve fiber density. While nerve function and structure deficits are assumed to directly correlate, thermal nociception does not necessarily occur in conjunction with small sensory nerve fiber loss and vice versa (Shun et al., 2004; Kennedy et al., 1996). For example, in one prior study, a decrease in intraepidermal nerve fiber density in the foot skin of diabetic mice occurred much later than onset of thermal hypoalgesia (Beiswenger et al., 2008). Moreover, studies that analyzed corneal nerve density in animal models with peripheral neuropathy have even reported brief increases in nerve density prior to a dramatic decrease in nerve fiber density as disease progresses (Chen et al., 2014). The deficits in small fiber function of the F35 mice and 93N mice are unlikely to be due to loss of nerve density per se.

Future experiments should investigate small C-fiber structural parameters analogous to those of large fibers. While nerve fiber density loss may contribute to thermal hypoalgesia, loss of thermal sensation may also be related to structural or functional Schwann cell abnormalities, decrease in axon caliber, or decreased sensory NCV. This approach is analogous to my previous large fiber structural analyses in the sciatic nerve. Electron microscopy can be used to analyze Schwann cells that surround small unmyelinated C-fibers to form Remak bundles. Analysis of Remak bundle structures can determine if Schwann cells proliferation is stunted or if a significant difference between the number Remak bundles per sciatic nerve in each group exists. Analysis of axonal caliber of small fibers can also determine if axonal shrinkage is occurring and contributes to small fiber NCV slowing, as observed in large efferent fibers.

Prion Protein Deposition and Neuropathy

Despite causing extensive peripheral and central nervous system dysfunction, a particularly interesting aspect of the 93N mouse model is the complete absence of protein aggregates, which appears to contradict the most widely held theory in prion research, in which protein aggregates are required for prion neurotoxicity. Indeed,

protein aggregates caused by misfolded proteins are especially common in most neurodegenerative disorders including, but not limited to, Parkinson's disease, Huntington's disease, Alzheimer's disease, and ALS (Ross and Poirier, 2004; Norrby, 2011; Marciniuk et al., 2013). However, as the 93N model shows no presence of protein aggregates in any tissue yet analyzed (Sigurdson Lab, Personal Communication, unpublished data), prion aggregates do not seem to contribute to the neurotoxic mechanism in either the central nervous system or the peripheral nervous system.

There may be some precedence for disassociation of protein deposition from neurotoxicity in other neurodegenerative diseases. For example, amyloid beta plaque deposits, a biomarker of Alzheimer's disease, do not differ in concentration between aging, non-demented elderly patients and dementia patients, despite claims that amyloid beta plaque leads to neuronal loss (Davis et al., 1999; Price et al., 2009). Therefore, amyloid beta plaques appear to be a part of normal aging, rather than the main Alzheimer's neurotoxic pathway. One may argue that without the hallmark protein aggregates, the prion disease modeled by the 93N mice cannot be considered a proteinopathy or a prion disease. Nonetheless, the 93N model represents an acquired prion disease as its disease state is caused by a mutant protein that leads to spongiform encephalopathy in the brain.

Sexual Dimorphism in Neurodegenerative Diseases

Sexual dimorphism in neurodegenerative diseases is characterized as sex differences in onset, clinical presentations, progression, and functional and structural abnormalities of the nervous system in neurodegenerative diseases. As such, sexual differences in neurological functions and structures presents a unique challenge in treating nervous system disorders and must be fully understood and explored to determine optimal treatment options and predicting disease progression for the estimated 1 billion individuals suffering from a form of neurodegenerative disorder (World Health Organization Reports, 2018). Brain tissues such as the hippocampus, the amygdala, and the cortex have shown sexual dimorphism in structure, responses to environmental stressors, and levels of neurotransmitters (Cahill, 2006; Yanguas-Casas, 2017). In neurodegenerative diseases such as Alzheimer's disease, neuronal density and the mitochondrial response to oxidative stress differs between sexes and brain regions in both humans and transgenic mouse models (Martinez-Pinilla et al., 2016; Djordjevic et al., 2017). Mouse models of diabetic neuropathy also show sexual differences in clinical presentations of neuropathic symptoms (O'Brien et al., 2017;

Pesaresi et al., 2018). Understanding sexual dimorphism in brain structure and function may explain seemingly random ranges in clinical symptoms, onset, and disease progression in neurodegenerative diseases.

In prion disease, sexual dimorphism in disease incubation time has been reported, although sexual dimorphic patterns are highly specific and only appear in certain combinations of mouse model and prion strain (Akhtar et al., 2011). The study by Akhtar et al. reveal significant sex differences in C57Bl/6 and FVB/NHsd mouse models in particular, in which female mice had shorter prion protein incubation times than those of male mice. Curiously, in BSE strains adapted for the mouse models, male mice showed shorter incubations times compared to female mice. Despite these differences in incubation time, levels of scrapie protein and histological features in brain tissue did not appear to differ between the sexes of any strain or for any mouse model.

Summary & Future Studies

Both F35 and 93N prion disease mouse models show evidence of axonal neuropathy. In characterizing their respective peripheral neuropathic symptoms, both F35 mice and 93N mice showed significant large motor dysfunction and small sensory fiber dysfunction without changes in total fiber density of either large fibers or small fibers. In large fibers, motor dysfunction in F35 and 93N mice was associated with reduced mean axonal diameter of myelinated fibers and axonal size-frequency distributions skewed towards smaller axonal calibers.

To complete analysis of small fiber function, I propose measuring mean sensory nerve conduction velocity for each group and, in conjunction, measuring levels of substance P and glutamate and their respective receptors to identify potential causes of small fiber dysfunction in the presence of normal nerve density. Additionally, I propose analyzing small fiber structures such as Remak bundles and their respective Schwann cells in the sciatic nerve using electron microscopy.

Future experiments examining aspects of myelination should also be implemented. Quantifying levels of MBP and myelin sheath area could confirm if changes in myelin have occurred alongside axonal atrophy and supplement lower g-ratio values in F35 and 93N mouse models. Measurements of internodal distance should also be performed to establish whether internodal differences contribute to MNCV slowing.

Supplemental revisions for this study should include more animals added to the study, especially female controls to further investigate the sexual dimorphic large myelinated fiber dysfunction in the 93N model.

Supplemental experiments to confirm prion disease in these mice models such as multiple rotarod testing over a duration of time to assess learning capacity or memory tests should also be performed. To further investigate the potential for the N-terminus of the prion protein as the main neurotoxic fragment, a similar study can be performed to compare N-terminus modified prion models and C-terminus modified prion models.

Ultimately, future studies may use F35 and 93N mice to assess efficacy of potential therapeutics that are currently being developed, such as anti-PrP antibodies (Burchell and Panegyres, 2016) and drugs that promote formation of new neurons from stem cells (Gage and Temple, 2013; McIntyre et al., 2017).

REFERENCES

Aaberg, M. L., Burch, D. M., Hud, Z. R., and Zacharias, M. P. (2008). Gender Differences in the Onset of Diabetic Neuropathy. Journal of Diabetes Complications, 22(2):83-7. http://doi: 10.1016/j.jdiacomp.2007.06.009.

Adlkofer, K., Martini, R., Aguzzi, A., Zielasek, J., Toyka, K. V., and Suter, U. (1995)

Aguzzi, A., Heikenwalder, M., and Polymenidou, M. (2007). Insights into prion strains and neurotoxicity. Nature reviews. Molecular Biology, 8(7):552-61.

Aguzzi, A., Heppner, F. L., Heikenwalder, M., Prinz, M., Mertz, K., Seeger, H., and Glatzel, M. (2003). Immune system and peripheral nerves in propagation of prions to CNS, British Medical Bulletin, 66(1):141–159. https://doi.org/10.1093/bmb/66.1.141.

Akhtar, S., Wenborn, A., Brandner S., Collinge J., and Lloyd S.E. (2011). Sex Effects in Mouse Prion Disease Incubation Time. PLoS ONE 6(12): e28741. https://doi.org/10.1371/journal.pone.0028741.

al-Ghoul, W. M., Li Volsi, G., Weinberg, R. J., Rustioni, A. (1993). Glutamate immunocytochemistry in the dorsal horn after injury or stimulation of the sciatic nerve of rats. 30(3-4):453-9.

Alper, T., Cramp, W. A., Haig, D. A., and Clarke, M. C. (1967). Does the agent of scrapie replicate without nucleic acid? Nature, 214(5090):764-6.

Alper, T., Haig, D. A., and Clarke, M. C. (1966). The exceptionally small size of the scrapie agent. Biochemical and biophysical research communications, 22(3):278-84.

Anderson, R. M., Donnelly, C. A., Ferguson, N. M., Woolhouse, M. E., Watt, C. J., Udy, H. J., MaWhinney, S., Dunstan, S. P., Southwood, T. R., Wilesmith, J. W., Ryan, J. B., Hoinville, L. J., Hillerton, J. e., Austin, A. R., and Wells, G. A. (1997). Nature, 386(6622):302.

Andrews, N. J., Farrington, C. P., Cousens, S. N., Smith, P. G., Ward, H., Knight, R. S., Ironside, J. W., and Will, R. G. (2000). Incidence of variant Creutzfeldt-Jakob disease in the UK. Lancet, 356(9228):481-2.

Asante, E. A., Linehan, J. M., Desbruslais, M., Joiner, S., Gowland, I., Wood, A. L., Welch, J., Hill, A. F., Lloyd, S. E., and Collinge, J. (2002). BSE prions propagate as either variant CJD-like or sporadic CJD-like prion strains in transgenic mice expressing human prion protein. The EMBO Journal, 21(23), 6358–6366. http://doi.org/10.1093/emboj/cdf653.

Baker, H. E., Poulter, M., Crow, T. J., Frith, C. D., Lofthouse, R., Ridley, R. M. (1991). Aminoacid polymorphism in human prion protein and age at death in inherited prion disease. Lancet, 337:1286 (letter).

Barria, M. A., Mukherjee, A., Gonzalez-Romero, D., Morales, R., and Soto, C. (2009). De novo generation of infectious prions in vitro produces a new phenotype. PloS Pathog., 5(5):e1000421.

Barry, D. M., Stevenson, W., Bober, B. G., Wiese, P. J., Dale, J. M., Barry, G. S., Byers, N. S., Strope, J. D., Chang, R., Schulz, D. J., Shah, S., Calcutt, N. a., Gebremichael, Y. and Garcia, M. L. (2012). Expansion of NF-M carboxy terminus increases axonal diameter independent of increases in conduction velocity or myelin thickness. The Journal of Neuroscience, 32(18), 6209–6219. http://doi.org/10.1523/JNEUROSCI.0647-12.2012.

Baumann, F., Tolnay, M., Brabeck, C., Pahnke, J., Kloz, U., Niemann, H. H., Heikenwalder, M., Rulicke, T., Burkle, A., and Aguzzi, A. (2007). Lethal recessive myelin toxicity of prion protein lacking its central domain. The EMBO Journal, 26(2), 538–547. http://doi.org/10.1038/sj.emboj.7601510.

Baylis, M., Chihota, C., Stevenson, E., Goldmann, W., Smith, A., Sivam, K., Tongue, S., and Gravenor, M. B. (2004). Risk of scrapie in British sheep of different prion protein genotype. J Gen Virol., 85(Pt 9):2735-40.

Beck, E., Daniel, P. M., Matthews, W. B., Stevens, D. L., Alpers, M. P., Asher, D. M., Gajdusek, D. C., and Gibbs, C. J., Jr. (1969). Creutzfeldt-Jakob disease: the neuropathology of a transmission experiment. Brain: a journal of neurology, 92(4):699-716.

Beiswenger, K. K., Calcutt, N. A., & Mizisin, A. P. (2008). Dissociation of Thermal Nociception and Epidermal Innervation in Streptozotocin-Diabetic Mice. Neuroscience Letters, 442(3), 267–272. http://doi.org/10.1016/j.neulet.2008.06.079.

Belay, E. D. (1999). Transmissible spongiform encephalopathies in humans. Annu Rev Microbiol., 53():283-314.

Belyantseva, I. A. and Lewin, G. R. (1999). Stability and plasticity of primary afferent projections following nerve regeneration and central degeneration. The European Journal of Neuroscience, 11(2):457-68.

Benestad, S. L., Arsac, J. N., Goldmann, W., and Noremark, M.(2008). Atypical/Nor98 scrapie: properties of the agent, genetics, and epidemiology. Vet Res, 39:19. 10.1051/vetres:2007056.

Berger, Z., Smith, K. A., & LaVoie, M. J. (2010). Membrane localization of LRRK2 is associated with increased formation of the highly active LRRK2 dimer and changes in its phosphorylation. Biochemistry, 49(26), 5511–5523. http://doi.org/10.1021/bi100157u.

Bianca, M., Bianca, S., Vecchio, I., Raffaele, R., Ingegnosi, C., Nicoletti, F. (2003). Gerstmann-Straussler-Scheinker disease with P102L-V129 mutation: a case with psychiatric manifestations at onset. Annals of Genetics, 46(4):467-9.

Bierhaus, A., Schiekofer, S., Schwaninger, M., Andrassy, M., Humper, P. M., Chen, J., Hong, M., Luther, T., Henle, T., Kloting, I., Morcos, M., Hofmann, M., Tritschler, H., Weigie, B., Kasper, M., Smith, M., Perry, G., Schmidt, A. M., Stern, D. M., Haring, H. U., Schleicher, E., and Nawroth, P. P. (2001). Journal of Diabetes, 50(12):2792-808.

Bosch, X. (2001). UK drug company's vCJD infected drug causes chaos in Spain. Lancet;357(9256):618.

Bouybayoune, I., Mantovani, S., Del Gallo, F., Bertani, I., Restelli, E., Comerio, L., Tapella, L., Baracchi, F., Fernandez-Borges, N., Mangieri, M., Bisighini, C., Beznoussenko, G. V., Paladini, A., Balducci, C., Micotti, E., Forloni, G., Castilla, J., Fiordaliso, F., Tagliavini, F., Imeri, L., and Chiesa, R. (2015). Transgenic Fatal Familial Insomnia Mice Indicate Prion Infectivity-Independent Mechanisms of Pathogenesis and Phenotypic Expression of Disease. PLoS Pathogens, 11(4), e1004796. http://doi.org/10.1371/journal.ppat.1004796.

Braak, H. & Del Tredici, K. Acta Neuropathol (2014) 128: 767. https://doi.org/10.1007/s00401-014-1356-1.

Bradner, S. and Jaunmuktane, Z. (2017). Prion disease: experimental models and reality. Acta Neuropathol., 133(2):197-222. doi: 10.1007/s00401-017-1670-5.

Brandel, J. P. (2004). Transmissible spongiform encephalopathies. Orphanet Encyclopedia, pp. 1-7. http://www.orpha.net/data/patho/GB/uk-TSE.pdf.

Bremer, J., Baumann, F., Tiberi, C., Wessig, C., Fischer, H., Schwarz, P., Steele, A. D., Toyka, K. V., Nave, K. A., Weis, J., and Aguzzi, A., (2010). Axonal prion protein is required for peripheral myelin maintenance. Nature Neuroscience, 13(3):310-8. doi: 10.1038/nn.2483.

Brill, M. H., Waxman, S. G., Moore, J. W., and Joyner, R. W. (1977). Conduction velocity and spike configuration in myelinated fibres: computer dependence on internodal distance. 40(8):769-74.

Brown, K., and Mastrianni, J. A. (2010). The prion diseases. J Geriatr Psychiatry Neurol. 23(4):277-98.

Brown, P., Cathala, F., Raubertas, R. F., Gajdusek, D. C., Castaigne, P. (1987). The epidemiology of Creutzfeldt-Jakob disease: conclusion of a 15-year investigation in France and review of the world literature. Neurology, 37:895-904.

Bruce, M. E., Will, R. G., Ironside, J. W., McConnell, I., Drummond, D., Suttie, A., McCardie, L., Chree, A., Hope, J., Birkett, C., Cousens, S., Fraser, H., and Bostock, C. J. (1997). Transmissions to mice indicate that 'new variant' CJD is caused by the BSE agent. Nature, 389(6650):498-501.

Bueler, H., Aguzzi, A., Sailer, A., Greiner, R. A., Autenried, P., Aguet, M., and Weissman, C. (1993). Cell, 73(7):1339-47.

Burchell, J. T., & Panegyres, P. K. (2016). Prion diseases: immunotargets and therapy. ImmunoTargets and Therapy, 5, 57–68. http://doi.org/10.2147/ITT.S64795.

Cahill, L. (2006). Why sex matters for neuroscience. Nature Reviews Neuroscience, 7:477-484.

Campos, F. L., Carvalho, M. M., Cristovão, A. C., Je, G., Baltazar, G., Salgado, A. J., Kim Y. S., and Sousa, N. (2013). Rodent models of Parkinson's disease: beyond the motor symptomatology. Frontiers in Behavioral Neuroscience, 7, 175. http://doi.org/10.3389/fnbeh.2013.00175.

Capellari, S., Stramiello, R., Saverioni, D., Kretzschmar, H., Parchi, P. (2011). Genetic Creutzfeldt-Jakob disease and fatal familial insomnia: insights into phenotypic variability and disease pathogenesis. Acta Neuropathol., 121(1):21-37.

Capucchio, M. T., Guarda, F., Pozzato, N., Coppolino, S., Caracappa, S., Di Marco, V. (2001). Clinical signs and diagnosis of scrapie in Italy: a comparative study in sheep and goats. J Vet Med A Physiol Pathol Clin Med., 48(1):23-31.

Carroll, J. A., Striebel, J. F., Race, B., Phillips, K., and Chesebro, B. (2015). Prion Infection of Mouse Brain Reveals Multiple New Upregulated Genes Involved in Neuroinflammation or Signal Transduction. Journal of Virology, 89(4), 2388–2404. http://doi.org/10.1128/JVI.02952-14.

Carroll, J. A., Striebel, J. F., Rangel, A., Woods, T., Phillips, K., Peterson, K. E., Race B., and Chesebro, B. (2016). Prion Strain Differences in Accumulation of PrPSc on Neurons and Glia Are Associated with Similar Expression Profiles of Neuroinflammatory Genes: Comparison of Three Prion Strains. PLoS Pathogens, 12(4), e1005551. http://doi.org/10.1371/journal.ppat.1005551.

Caughey B, and Baron, G. S. (2006). Prions and their partners in crime. Nature, 443(7113):803-10.

Center for Food and Safety. (2018). Timeline of Mad Cow Disease Outbreaks.

Chandler, R. L. (1961). Encephalopathy in mice produced by inoculation with scrapie brain material. Lancet, 1(7191):1378-9.

Chapuis, J., Moudjou, M., Reine, F., Herzog, L., Jaumain, E., Chapuis, C., … Béringue, V. (2016). Emergence of two prion subtypes in ovine PrP transgenic mice infected with human MM2-cortical Creutzfeldt-Jakob disease prions. Acta Neuropathologica Communications, 4, 10. http://doi.org/10.1186/s40478-016-0284-9.

Cheah, M., Fawcett, J. W., & Andrews, M. R. (2017). Assessment of Thermal Pain Sensation in Rats and Mice Using the Hargreaves Test. Bio-Protocol, 7(16), e2506. http://doi.org/10.21769/BioProtoc.2506.

Chen, D. K., Frizzi, K. E., Guernsey, L. S., Ladt, K., Mizisin, A. P., & Calcutt, N. A. (2013). Repeated monitoring of corneal nerves by confocal microscopy as an index of peripheral neuropathy in type-1 diabetic rodents and the effects of topical insulin. Journal of the Peripheral Nervous System : JPNS, 18(4), 306–315. http://doi.org/10.1111/jns5.12044.

Chen, S. G., Teplow, D. B., Parchi, P., Teller, J. K., Gambetti, P., Autilio-Gambetti, L. (1995). Truncated forms of the human prion protein in normal brain and in prion diseases. Journal of Biological Chemistry, 270(32):19173-80.

Chen, X., Graham, J., Dabbah, M. A., Petropoulos, I. N., Ponirakis, G., Asghar, O., Uazman, A., Marshall, A., Fadayi, H., Ferdousi, M., Azmi, S., Tavakoli, M., Efron, N., Jeziorska, M., and Malik, R. A. (2015). Small Nerve Fiber Quantification in the Diagnosis of Diabetic Sensorimotor Polyneuropathy: Comparing Corneal Confocal Microscopy With Intraepidermal Nerve Fiber Density. Diabetes Care, 38(6), 1138–1144. http://doi.org/10.2337/dc14-2422.

Chomiak, T., & Hu, B. (2009). What Is the Optimal Value of the g-Ratio for Myelinated Fibers in the Rat CNS? A Theoretical Approach . PLoS ONE, 4(11), e7754. http://doi.org/10.1371/journal.pone.0007754.

Cornealius, J. R., Boes, C. J., Ghearing, G., Leavitt, J. A., Kumar, N. (2009). Visual symptoms in the Heidenhain variant of Creutzfeldt-Jakob Disease. Journal of Neuroimaging, 19(3):283-7.

Coull JA, Beggs S, Boudreau D, Bolvin D, Tsuda M, Inoue K, Gravel C, Salter MW, De Koninck Y. (2005). Nature, 438(7070):1017-21.

Crozet, C., Lezmi, S., Flamant, F., Samarut, J., Baron, T., and Bencsik A. (2007). Peripheral circulation of the prion infectious agent in transgenic mice expressing the ovine prion protein gene in neurons only. Journal of Infectious Diseases, 195(7):997-1006.

Cuille, J, and Chelle, P. L. (1939). Experimental transmission of trembling to the goat. C. R. Seances Acad Sci., 208:1058-1160.

Davis, D. G., Schmitt, F. A., Wekstein, D. R., and Markesbery, W. R. (1999). Alzheimer neuropathologic alterations in aged cognitively normal subjects.Journal of Neuropathology and Experimental Neurology, 58(4):376-88.

de La Hoz., C. L., Cheng C., Fernyhough P., and Zochodne D. W. (2017). A Model of Chronic Diabetic Polyneuropathy: Benefits from Intranasal Insulin Modified by Sex and RAGE Deletion. American Journal of Physiology and Endocrinology Metabolism, b 312: E407–E419. http:// doi:10.1152/ajpendo.00444.2016.

Deleault, N. R., Geoghegan, J. C., Nishina, K., Kascsak, R., Williamson, R. A., and Supattapone, S. (2005). Protease-resistant prion protein amplification reconstituted with partially purified substrates and synthetic polyanions. J Biol Chem, 280(29):26873-9.

Deuis, J. R., Dvorakova, L. S., & Vetter, I. (2017). Methods Used to Evaluate Pain Behaviors in Rodents. Frontiers in Molecular Neuroscience, 10, 284. http://doi.org/10.3389/fnmol.2017.00284.

Dickinson, A. G., Meikle, V. M., and Fraser, H. (1968). Identification of a gene which controls the incubation period of some strains of scrapie agent in mice. Journal of comparative pathology, 78(3):293-299.

Djordjevic, J., Thomson, E., Chowdhury, S. R., Snow W. M., Perez, C., Wong, T. P., Ferneyhough, P., Albensi, B. C. (2017). Brain region- and sex-specific alterations in mitochondrial function and NF-kB signaling in the TgCRND8 mouse model of Alzheimer's disease. Journal of Neuroscience, 361:81-92. doi: 10.1016/j.neuroscience.2017.08.006.

Dossena, S., Imeri, L., Mangieri, M., Garofoli, A., Ferrari, L., Senatore, A., Restelli, E., Balducci, C., Fiordaliso, F., Salio, M., Bianchi, S., Fioriti, L., Morbin, M., Pincherle, A., Marcon, G., Villani, F., Carli, M., Tagliavini, F., Forloni, G., and Chiesa, R. (2008). Mutant prion protein expression causes motor and memory deficits and abnormal sleep patterns in a transgenic mouse model. Neuron, 60(4):598-609, doi: 10.1016/j.neuron.2008.09.008.

Doubell, T. P., Mannion, R. J., and Woolf, C. J. (1997). Intact sciatic myelinated primary afferent terminals collaterally sprout in the adult rat dorsal horn following section of a neighbouring peripheral nerve. The Journal of Comparative Neurology, 380(1):95-104.

Ducrot, C., Arnold, M., de Koeijer, A., Heim, D., and Calavas, D. (2008). Review on the epidemiology and dynamics of BSE epidemics. Vet Res, 39:15. 10.1051/vetres:2007053.

Elliott, J., Tesfaye, S., Chaturvedi, N., Gandhi, R. A., Stevens, L. K., Emery, C., and Fuller, J. H. on behalf of the EURODIAB Prospective Complications Study Group. (2009). Large-Fiber Dysfunction in Diabetic Peripheral Neuropathy Is Predicted by Cardiovascular Risk Factors. Diabetes Care, 32(10), 1896–1900. http://doi.org/10.2337/dc09-0554.

Favereaux A, Quadrio I, Vital C, et al. Pathologic Prion Protein Spreading in the Peripheral Nervous System of a Patient With Sporadic Creutzfeldt-Jakob Disease. Arch Neurol. 2004;61(5):747–750. doi:10.1001/archneur.61.5.747.

Fields, R.D. (2008). White matter in learning, cognition and psychiatric disorders. Trends Neurosci., 31(361-370), 10.1016/j.tins.2008.04.001.

Fischer, M., Rülicke, T., Raeber, A., Sailer, A., Moser, M., Oesch, B., Brandner, S., Aguzzi, A., and Weissmann, C. (1996). Prion protein (PrP) with amino-proximal deletions restoring susceptibility of PrP knockout mice to scrapie. The EMBO Journal, 15(6), 1255–1264.

Flechsig E, Hegyi I, Enari M, Schwarz P, Collinge J, and Weissmann C. (2001). Transmission of scrapie by steel-surface-bound prions. Mol Med, 7:679–84.

Flechsig, E., Shmerling, D., Hegyi, I., Raeber, A. J., Fischer, M., Cozzio, A., von Mering, C., Aguzzi, A., Weissman, C. (2000). Prion protein devoid of the octapeptide repeat region restores susceptibility to scrapie in PrP knockout mice. Neuron, 27(2):399-408.

Fleming, S. M., Ekhator, O. R., & Ghisays, V. (2013). Assessment of Sensorimotor Function in Mouse Models of Parkinson's Disease. Journal of Visualized Experiments: JoVE, (76), 50303. Advance online publication. http://doi.org/10.3791/50303.

Gage, F. H., Temple, S. (2013). Neural stem cells: generating and regenerating the brain. Neuron, 80(3):588-601. DOI: https://doi.org/10.1016/j.neuron.2013.10.037.

Gambetti, P., Kong, Q., Zou, W., Parchi, P., Chen, S. G. (2003). Sporadic and familial CJD: classification and characterization. British Medical Bulletin, 66(1):213-219, doi./10.1093/bmb/66.1.213.

Gasser H.S., Grundfest H. (1939). Axon diameters in relation to the spike dimensions and the conduction velocity in mammalian A fibres. Brain Res; 127:393–414.

Gibbs, C. J., Jr., Gajdusek, D. C., Asher, D. M., Alpers, M. P., Beck, E., Daniel, P. M., and Matthews, W. B. (1968). Creutzfeldt-Jakob disease (spongiform encephalopathy): transmission to the chimpanzee. Science, 161(3839):388-9.

Glatzel, M., Giger, O., Braun, N., and Aguzzi, A. (2004). The peripheral nervous system and the pathogenesis of prion diseases. Current molecular medicine, 4(4):355-9.

Goldmann, W. (2008). PrP genetics in ruminant transmissible spongiform encephalopathies. Vet Res, 39:30. 10.1051/vetres:2008010.

Gravenor MB, Cox DR, Hoinville LJ, Hoek A, McLean AR. (2000). Scrapie in Britain during the BSE years. Nature, 406(6796):584–5.

Griffith, J. S. (1967). Self-replication and scrapie. Nature, 215(5105):1043-4.

Hadlow, W. J. (2008). Kuru likened to scrapie: the story remembered. Philosophical Transactions of the Royal Society B: Biological Sciences, 363(1510), 3644. http://doi.org/10.1098/rstb.2008.4013.

Hadlow, W.J. (1959). Scrapie and kuru. Lancet, 289–290.

Hargreaves, K., Dubner, R., Brown, F., Flores, C., and Joris, J. (1988). A new and sensitive method for measuring thermal nociception in cutaneous hyperalgesia. Journal of Pain, 32(1):77-88.

Harris, D. A., Huber, M. T., van Dijken, P., Shyng, S. L., Chait, B. T., Wang, R. (1993). Processing of a cellular prion protein: identification of N- and C-terminal cleavage sites. Biochemistry, 32(4):1009-16.

Harris, J. A., Corsi, M., Quartaroli, M., Arban, R., Bentivoglio, M. (1996). Upregulation of spinal glutamate receptors in chronic pain. Neuroscience. 74(1):7-12.

Hauw, J. J., Sazdovitch, V., Laplanche, J. L., Peoc'h, K., Kopp, N., Kemeny, J., Privat, N., Delasnerie-Laupretre, N., Brandel, J. P., Desiys, J. P., Dormont, D., Alperovitch, A. (2000). Neurology, 54(8):1641-6.

Heaton, M. P., Keele, J. W., Harhay, G. P., Richt, J. A., Koohmaraie, M., Wheeler, T. L., Shackelford, S. D., Casas, E., King, D. A., Sonstegard, T. S., Van Tassell, C. P., Neibergs, H. L., Chase, C. C. Jr., Kalbfleisch, T. S., Smith, T. P. L., Clawson, M. L., Laegreid, W. W. (2008). Prevalence of prion protein gene E211K variant in U. S. cattle. BMC Vet Res, 4:25. 10.1186/1746-6148-4-25.

Heikenwalder, M., Julius, C., and Aguzzi, A. (2007). Journal of Neuroscience Research, 85(12):2714-25.

Heske, J., Heller, U., Winklhofer, K. F., Tatzelt, J. (2003) The C-terminal globular domain of the prion protein is necessary and sufficient for important into the endoplasmic reticulum. The Journal of Biological Chemistry, 279, 5433-5443, doi: 10.1074/jbc.M309570200.

Hill, A. F., Butterworth, R. J., Joiner, S., Jackson, g., Rossor, M. N., Thomas, D. J., Frosh, A., Toiley, N., Bell, J. E., Spencer, M., King, A., Al-Sarraj, S., Ironside, J. W., Lantos, P. L., and Collinge, J. (1999). Investigation of variant Creutzfeldt-Jakob disease and other human prion diseases with tonsil biopsy samples. Lancet, 353:183-9.

Hill, A. F., Desbruslais, M., Joiner, S., Sidle, K. C., Gowland, I., Collinge, J., Doey, L. J., Lantos, P. (1997). The same prion strain causes vCJD and BSE. Nature, 389:448-450,526. doi: 10.1038/38925.

Hunter, G. D. and Millson, G. C. (1964). Studies on the heat stability and chromatographic behavior of the scrapie agent. Journal of General Microbiology, 37:251-8.

Imran, M., & Mahmood, S. (2011). An overview of human prion diseases. Virology Journal, 8, 559. http://doi.org/10.1186/1743-422X-8-559.

Ishida, C., Okino, S., Kitamoto, T., & Yamada, M. (2005). Involvement of the peripheral nervous system in human prion diseases including dural graft associated Creutzfeldt–Jakob disease. Journal of Neurology, Neurosurgery, and Psychiatry, 76(3), 325–329. http://doi.org/10.1136/jnnp.2003.035154.

Iwasaki, Y., Yoshida, M., Hashizume, Y., Kitamoto, T., Sobue, G. (2006). Clinicopathologic characteristics of sporadic Japanese Creutzfeldt-Jakob disease classified according to prion protein gene polymorphism and prion protein type. Acta Neuropathol., 112(5):561-71.

Jackson, W. S., Borkowski, A. W., Watson, N. E., King, O. D., Faas, H., Jasanoff, A., & Lindquist, S. (2013). Profoundly different prion diseases in knock-in mice carrying single PrP codon substitutions associated with human diseases. Proceedings of the National Academy of Sciences of the United States of America, 110(36), 14759–14764. http://doi.org/10.1073/pnas.1312006110.

Jacobs, J. G., Langeveld, J. P., Biacabe, A. G., Acutis, P. L., Polak, M. P., Gavier-Widen, D., Buschmann, A., Caramelli, M., Casalone, C., Mazza, M., Groschup, M., Erkens, J. H., Davidse, A., van Zijderveld, F. G., and Baron, T. (2007). Molecular discrimination of atypical bovine spongiform encephalopathy strains from a geographical region spanning a wide area in Europe. Journal of Clinical Microbiology, 45(6):1821-9.

Jakobsen, J., Brimijoin, S., and Sidenius, P. (1983). Axonal transport in neuropathy. Muscle and Nerve, 6(2):164-166. doi: 10.1002/mus.880060214.

Jeffrey, M., González, L. (2007). Classical sheep transmissible spongiform encephalopathies: pathogenesis, pathological phenotypes and clinical disease. Neuropathol Appl Neurobiol, 33: 373-394. 10.1111/j.1365-2990.2007.00868.

Jeffrey, M., Goodsir, C., McGovern, G., Barmada, S. J., Medrano, A. Z., & Harris, D. A. (2009). Prion Protein with an Insertional Mutation Accumulates on Axonal and Dendritic Plasmalemma and Is Associated with Distinctive Ultrastructural Changes. The American Journal of Pathology, 175(3), 1208–1217. http://doi.org/10.2353/ajpath.2009.090125.

Jensen, T. S., Finnerup, N. B. (2014). Allodynia and hyperalgesia in neuropathic pain: clinical manifestations and mechanisms. The Lancet Neurology, 13(9): 924-935. doi:10.1016/S1474-4422(14)70102-4.

Johnson, K. A., Schultz, A., Betensky, R. A., Becker, J. A., Sepulcre, J., Rentz, D., Mormino, E., Chhatwal, J., Amariglio, R., Papp, K., Marshall, G., Albers, M., Mauro, S., Pepin, L., Alverio, J., Judge, K., Philiossaint, M., Shoup, T., Yokell, D., Dickerson, B., Gomez-Isla, T., Hyman, B., Vasdev, N., and Sperling, R. (2016). Tau PET imaging in aging and early Alzheimer's disease. Annals of Neurology, 79(1), 110–119. http://doi.org/10.1002/ana.24546.

Jolivalt, C. G., Frizzi, K. E., Guernsey, L., Marquez, A., Ochoa, J., Rodriguez, M., & Calcutt, N. A. (2016). PHENOTYPING PERIPHERAL NEUROPATHY IN MOUSE MODELS OF DIABETES. Current Protocols in Mouse Biology, 6(3), 223–255. http://doi.org/10.1002/cpmo.11.

Journal of the House of Commons. 1755. p. 27. :87.

Juling, K., Schwarzenbacher, H., Williams, J. L., Fries, R. (2006). A major genetic component of BSE susceptibility. BMC Biology, 4:33. 10.1186/1741-7007-4-33.

Kambiz, S., van Neck, J. W., Cosgun, S. G., van Velzen, M. H. N, Joop, A. M., Janssen, J. L., Avazverdi, N.,Hovius, S. E. R., Walbeehm, E. T. (2015) Correction: An Early Diagnostic Tool for Diabetic Peripheral Neuropathy in Rats. PLOS ONE 10(6): e0131144. https://doi.org/10.1371/journal.pone.0131144.

Kennedy, W. R., Wendelschafer-Crabb, G., & Johnson, T. (1996). Quantitation of epidermal nerves in diabetic neuropathy. Neurology, 47(4), 1042-1048.

Khan, G. M., Chen, S.-R., and Pan, H.-L. (2002). Role of primary afferent nerves in allodynia caused by diabetic neuropathy in rats. Journal of Neuroscience, 114(2), 291-299. https://doi.org/10.1016/S0306-4522(02)00372-X.

Klatzo, I., Gajdusek, D. C., and Zigas, V. (1959). Pathology of Kuru. Laboratory Investigation: a journal of technical methods and pathology, 8(4):799-847.

Kong, Q. K., Surewicz, W. K., Petersen, R. B., Zhou, W., Chen, S. G., Gambetti, P., Parchi, P., Capellari, S., Goldfarb, L., Montagna, P., Lugaresi, E., Piccardo, P., Ghetti, B. (2004). Prion Biology and Disease. 2nd edition, Cold Spring Harbor: Cold Spring Harbor Laboratory Press. pp. 673-776.

Konold, T., Davis, A., Bone, G., Bracegirdle, J., Everitt, S., Chaplin, M., … Simmons, M. M. (2007). Clinical findings in two cases of atypical scrapie in sheep: a case report. BMC Veterinary Research, 3, 2. http://doi.org/10.1186/1746-6148-3-2.

Kramer HH, Rolke R, Bickel A, Birklein F (2004a) Thermal thresholds predict painfulness of diabetic neuropathies. Diabetes Care, 27:2386–2391.

Kunt, T., Forst, T., Schmidt, S., Pfutzner, A., Schneider, S., Harzer, O., Lobig, M., Engelbach, M., Goitom, K., Pohlmann, T., and Beyer, J. (2000). Serum levels of substance P are decreased in patients with type 1 diabetes.

Lasmezas, C. I., Comoy, E., Hawkins, S., Herzog, C., Mouthon, F., Konold, T., Auvre, F., Correia, E., Lescoutra-Etchegaray, N., Sales, N, Wells, G., Brown, P., and Deslys, J. P. (2005). Risk of oral infection with bovine spongiform encephalopathy agent in primates. Lancet., 365(9461):781-3.

Lasmezas, C. I., Deslys, J. P., Demaimay, R., Adjou, K. T., Lamoury, F., Dormont, D., Robain, O., Ironside, J., Hauw, J. J. (1996). BSE transmission to macaques. Nature, 381:743-744. doi: 10.1038/381743a0.

Li, A., Piccardo, P., Barmada, S. J., Ghetti, B., & Harris, D. A. (2007). Prion protein with an octapeptide insertion has impaired neuroprotective activity in transgenic mice. The EMBO Journal, 26(11), 2777–2785. http://doi.org/10.1038/sj.emboj.7601726.

Lugaresi, E., Medori, R., Montagna, P., Baruzzi, A., Cortelli, P, Lugaresi, A., Tinuper, P., Zucconi, M., and Gambetti, P. (1986). Fatal familial insomnia and dysautonomia with selective degeneration of thalamic nuclei. The New England Journal of Medicine, 315(16):997-1003. doi: 10.1056/NEJM198610163151605.

Mabbott, N. A. (2017). How do PrPSc Prions Spread between Host Species, and within Hosts? Pathogens, 6(4), 60. http://doi.org/10.3390/pathogens6040060.

Maddison BC, Rees HC, Baker CA, Taema M, Bellworthy SJ, Thorne L, Terry LA, and Gough KC. (2010). Prions are secreted into the oral cavity in sheep with preclinical scrapie. J Infect Dis, 201: 1672-1676. 10.1086/652457.

Marciniuk, K., Taschuk, R., & Napper, S. (2013). Evidence for Prion-Like Mechanisms in Several Neurodegenerative Diseases: Potential Implications for Immunotherapy. Clinical and Developmental Immunology, 2013, 473706. http://doi.org/10.1155/2013/473706.

Marsh, R. F. (1992). Transmissible mink encephalopathy. In: Prusiner, S. B., Collinge, J., Powell, J., Anderton, B., eds. Prion disease in humans and animals. London: Ellis Horwood, 2:300-7.

Martínez-Pinilla, E., Ordóñez, C., del Valle, E., Navarro, A., & Tolivia, J. (2016). Regional and Gender Study of Neuronal Density in Brain during Aging and in Alzheimer's Disease. Frontiers in Aging Neuroscience, 8, 213. http://doi.org/10.3389/fnagi.2016.00213.

Masujin, K., Shu, Y., Yamakawa, Y

McDonald, A. J., Wu, B., & Harris, D. A. (2017) An inter-domain regulatory mechanism controls toxic activities of PrPC, Prion, 11:6, 388-397, DOI: 10.1080/19336896.2017.1384894.

McGowan, J. P. (1992). Scrapie in Sheep. Scott J Agric, 5:365-75.

McIntyre, R. S., Johe, K., Rong, C., Lee, Y. (2017). The neurogenic compound, NSI-189 phosphate: a novel multi-domain treatment capable of pro-cognitive andantidepressant effects. Expert Opinion on Investigation Drugs, 26(6):767-770. doi: 10.1080/13543784.2017.1324847.

Meggendorfer F. (1930) Klinische und genealogische Beobachtungen bei einem Fall von spastischer Pseudokosklerose Jakobs. Z Neurol Psychiatry; 128: 337–41. doi:10.1007/BF02864269.

Millhauser, G. L. (2004). Copper binding in the prion protein. Acc Chem Res., 37(2):79-85.

Monari, L., Chen, S. G., Brown, P., Parchi, P., Petersen, R. B., Mikol., J., Gray, F., Cortelli, P., Montagna, P., and Ghetti, B. (1994). Fatal familial insomnia and familial Creutzfeldt-Jakob disease: different prion proteins determined by a DNA polymorphism. Proc Natl Acad Sci U S A., 91(7):2839-42.

Montagna, P., Gambetti, P., Cortelli, P., Lugaresi, E. (2003). Familial and sporadic fatal insomnia. Lancet Neurology, 2(3):167-76.

Morell P, Quarles RH. (1999). The Myelin Sheath. In: Siegel GJ, Agranoff BW, Albers RW, et al., editors. Basic Neurochemistry: Molecular, Cellular and Medical Aspects. 6th edition. Philadelphia: Lippincott-Raven. Available from: https://www.ncbi.nlm.nih.gov/books/NBK27954/.

Morelli, K. H., Seburn, K. L., Schroeder, D. G., Spaulding, E. L., Dionne, L. A., Cox, G. A., & Burgess, R. W. (2017). Severity of Demyelinating and Axonal Neuropathy Mouse Models Is Modified by Genes Affecting Structure and Function of Peripheral Nodes. Cell Reports, 18(13), 3178–3191. http://doi.org/10.1016/j.celrep.2017.03.009.

Namavari, A., Chaudhary, S., Sarkar, J., Yco, L., Patel, K., Han, K. Y., Yue, B. Y., Chang, J.-H., and Jain, S. (2011). In Vivo Serial Imaging of Regenerating Corneal Nerves after Surgical Transection in Transgenic Thy1-YFP mice. Investigative Ophthalmology & Visual Science, 52(11), 8025–8032. http://doi.org/10.1167/iovs.11-8332.

National CJD Research and Surveillance Unit (2017). Creutzfeldt-Jakob disease in the UK. http://www.cjd.ed.ac.uk. Accessed on August 3, 2018.

National Institute of Neurological Disorders and Stroke (2018). Peripheral Neuropathy Fact Sheet. https://www.ninds.nih.gov/Disorders/Patient-Caregiver-Education/Fact-Sheets/Peripheral-Neuropathy-Fact-Sheet. Accessed on August 3, 2018.

Nazor, K. E., Seward, T., & Telling, G. C. (2007). Motor behavioral and neuropathological deficits in mice deficient for normal prion protein expression. Biochimica et Biophysica Acta, 1772(6), 645–653. http://doi.org/10.1016/j.bbadis.2007.04.004.

Neeper, M., Schmidt, A. M., Brett, J., Yan, S. D., Wang, F., Pan, Y. C., Elliston, K., Stern, D., and Shaw, A. (1992). Journal of Biological Chemistry, 267(21):14998-5004.

Neufield, M. Y., Josiphov, J., and Korczyn, A. D. (1992). Demyelinating peripheral neuropathy in Creutzfeldt-Jakob disease. Muscle and Nerve, 15(11):1234-9.

Nicholson, E. M., Brunelle, B. W., Richt, J. A., Kehril, M. E., Jr., Greenlee, J. J. (2008). Identification of a heritable polymorphism in bovine PRNP associated with genetic transmissible spongiform encephalopathy: evidence of heritable BSE. Plos ONE, 3:e2912. 10.1371/journal.pone.0002912.

Niewiadomska M, Kulczycki J, Wochnik-Dyjas D, Szpak, G. M., Rakowicz, M., Lojkowska, W., Niedzielska, K., Inglot, E., Wieclawska, M., Glazowski, C., and Tarnowska-Dziduszko, E. (2002). Impairment of the Peripheral Nervous System in Creutzfeldt-Jakob Disease. Arch Neurol, 59(9):1430–1436. doi:10.1001/archneur.59.9.1430.

Norrby, E. (2011). Prions and protein-folding diseases. Journal of Internal Medicine, 70(1):1-14. doi: 10.1111/j.1365-2796.2011.02387.

Novakofski, J., Brewer, M. S., Mateus-Pinilla, N., Killefer, J., and McCusker, R. H. (2005). Prion biology relevant to bovine spongiform encephalopathy. J Anim Sci, 83:1455-1476.

O'Brien, P. D., Hur, J., Robell, N. J., Hayes, J. M., Sakowski, S. A., & Feldman, E. L. (2016). Gender-specific differences in diabetic neuropathy in BTBR ob/ob mice. Journal of Diabetes and Its Complications, 30(1), 30–37. http://doi.org/10.1016/j.jdiacomp.2015.09.018.

Oesch, B., Westaway, D., Walchli, M., McKinley, M. P., Kent, S. B., Aebersold, R., Barry, R. A., Tempst, P., Teplow, D. B., and Hood, L. E. (1985). Cell, 40(4):735-46.

Okada, H., Iwamaru, Y., Fukuda, S., Yokoyama, T., & Mohri, S. (2012). Detection of Disease-associated Prion Protein in the Optic Nerve and the Adrenal Gland of Cattle with Bovine Spongiform Encephalopathy by Using Highly Sensitive Immunolabeling Procedures. Journal of Histochemistry and Cytochemistry, 60(4), 290–300. http://doi.org/10.1369/0022155412437218.

Oliveira-Soto, L., & Efron, N. (2001). Morphology of corneal nerves using confocal microscopy. Cornea, 20(4), 374-384.

O'Rourke KI, Zhuang D, Truscott TC, Yan H, Schneider DA: (2011). Sparse PrP-Sc accumulation in the placentas of goats with naturally acquired scrapie. BMC Vet Res, 7: 7. 10.1186/1746-6148-7-7.

Pallier, P. N., Drew, C. J., and Morton, A. J. (2009). The Detection and Measurement of Locomotor Deficits in a Transgenic Mouse Model of Huntington's Disease are task- and protocol- dependent: influence of non-motor factors on locomotor function. Brain research bulletin, 78(6):347-55. doi: 10.1016/j.brainresbull.2008.10.007.

Papanas, N., & Ziegler, D. (2013). Corneal confocal microscopy: a new technique for early detection of diabetic neuropathy. Current diabetes reports, 13(4), 488-499.

Parchi, P., Castellani, R., Capellari, S., Ghetti, B., Young, K., Chen, S. G., Farlow, M., Dickson, D. W., Sima, A. A., Trojanowski, J. Q., Petersen, R. B., and Gambetti, P. (1996). Molecular basis of phenotypic variability in sporadic Creutzfeldt-Jakob disease. Annals of Neurology, 39(6):767-78.

Pattison, I. H. (1966). The relative susceptibility of sheep, goats, and mice to two types of the goat scrapie agent. Res Vet Sci., 7:207-212.

Pavelka M., Roth J. (2010) Structure of the Synaptic Terminal. In: Functional Ultrastructure. Springer, Vienna.

Pesaresi, M., Giatti, S., Spezzano, R., Romano, S., Diviccaro, S., Borsello, T., Mitro, N., Caruso, D., Garcia-Segura, L. M., and Melcangi, R. C. (2018). Axonal transport in a peripheral diabetic neuropathy model: sex-dimorphic features.

Pittenger, G. L., Ray, M., Burcus, N. I., McNutty, P., Basta, B., and Vinik, A. I. (2004). Intraepidermal nerve fibers are indicators of small-fiber neuropathy in both diabetic and nondiabetic patients. Journal of Diabetes Care, 27(8):1974-9.

Pocchiari M, Puopolo M, Croes EA, Budka H, Gelpi E, Collins S, Lewis V, Sutcliffe T, Gullivi A, Delasnerie-Laupretre N, Brandel JP, Alperovitch A, Zerr I, Poser S, Kretzschmar HA, Ladogana A, Rietvald I, Mitrova E, Martinez-Martin P, de Pedro-Cuesta J, Glatzel M, Aguzzi A, Cooper S, Mackenzie J, van Dujin CM, and Will RG. (2004) Predictors of survival in sporadic Creutzfeldt-Jakob disease and other human transmissible spongiform encephalopathies. Brain 127: 2348–2359.

Polydefkis M, Hauer P, Sheth S, Sirdofsky M, Griffin JW, McArthur JC (2004) The time course of epidermal nerve fibre regeneration: studies in normal controls and in people with diabetes, with and without neuropathy. Brain. 127:1606–1615.

Price, J. L., McKeel, D. W., Buckles, V. D., Roe, C. M., Xiong, C., Grundman, M., Hansen, L. A., Petersen, R. C., Parisi, J. E., Dickson, D. W., Smith, C. D., Davis, D. G., Schmitt, F. A., Markesbery, W. R., Kaye, J., Kurlan, R., Hulette, C., Kurland, B. F., Higdon, R., Kukull, W., and Morris, J. C. (2009). Neuropathology of Nondemented Aging: Presumptive Evidence for Preclinical Alzheimer Disease. Neurobiology of Aging, 30(7), 1026–1036. http://doi.org/10.1016/j.neurobiolaging.2009.04.002.

Pruisner, S. B. (1998). Prions. Proc Natl Acad Sci U. S. A., 95(23):13363-83.

Pruisner, S. B., Bolton, D. C., Groth, D. F., Bowman K. A., Cochran, S. P., and McKinley, M. P. (1982). Further purification and characterization of scrapie prions. Journal of Biochemistry, 21(26):6942-50.

Pruisner, S. B., Groth, D., Serban, A., Koehler, R., Foster, D., Torchia, M., Burton, D., Yang, S. L., and DeArmond, S. J. (1993). Ablation of the prion protein (PrP) gene in mice prevents scrapie and facilitates production of anti-PrP antibodies. Proc Natl Acad Sci U S A, 90(22):10608-12.

Pruisner, S. B., McKinley, M. P., Bowman, K. A., Bolton, D. C., Bendheimer, P. E., Groth, D. F., and Glenner, G. G. (1983). Scrapie prions aggregate to form amyloid-like birefringent rods. Cell, 35(2 Pt 1):349-58.

Quattrini, C., Tavakoli, M., Jeziorska, M., Kallinikos, P., Tesfaye, S., Finnigan, J., Marshall, A., Boulton, A. J. M., Efron, N., and Malik, R. A. (2007). Surrogate Markers of Small Fiber Damage in Human Diabetic Neuropathy. Journal of Diabetes, 56(8): 2148-2154.https://doi.org/10.2337/db07-0285.

Ranvier, L. (1871). Contributions à l'histologie et à la physiologie des nerfs périphériques. Comptes Rendus de l'Académie des Sciences. 73:1168–1171.

Reihling, D. B., Levin, J. D. (2010). Pain and death: neurodegenerative disease mechanisms in the n

Richt, J. A., and Hall, S. M. (2008). BSE case associated with prion protein gene mutation. Plos Pathog, 4(9): e1000156. doi: 10.1371/journal.ppat.1000156.

Robinson, S. W., Nugent, M. L., Dinsdale, D., & Steinert, J. R. (2014). Prion protein facilitates synaptic vesicle release by enhancing release probability. Human Molecular Genetics, 23(17), 4581–4596. http://doi.org/10.1093/hmg/ddu171.

Rushton, W. A. H. (1951). A theory of the effects of fibre size in medullated nerve. The Journal of Physiology, 115(1), 101–122.

Sabatelli, M., Mignogna, T., Lippi, G., Servidel, S., Manfredi, G., Ricci, E., Bertini, E., Lo Monaco, M., Tonali, P. (1994). Autosomal recessive hypermyelinating neuropathy. Acta neuropathologica, 87(4):337-42.

Sabel, B. A. and Schneider, G.E. (1988). The principle of "conservation of total axonal arborizations": massive compensatory sprouting in the hamster subcortical visual system after early tectal lesions. Experimental Brain Research. 73(3):505-18.

Sander, P., Hamann, H., Pfeiffer, I., Wemheuer, W., Brenig, B., Groschup, M. H., Ziegler, U., Distl, O., Leeb, T. (2004). Analysis of sequence variability of the bovine prion protein gene (PRNP) in German cattle breeds. Neurogenetics, 5:19-25. 10.1007/s10048-003-0171-y.

Schindowski, K., Bretteville, A., Leroy, K., Bégard, S., Brion, J.-P., Hamdane, M., & Buée, L. (2006). Alzheimer's Disease-Like Tau Neuropathology Leads to Memory Deficits and Loss of Functional Synapses in a Novel Mutated Tau Transgenic Mouse without Any Motor Deficits. The American Journal of Pathology, 169(2), 599–616. http://doi.org/10.2353/ajpath.2006.060002.

Shmerling, D., Hegyi, I., Fischer, M., Blattler, T., Brandner, S., Gotz, J., Rulicke, T., Flechsig, E., Cozzio, A., von Mering, C., Hangartner, C., Aguzzi, A., and Weissman, C. (1998). Expression of amino-terminally truncated PrP in the mouse leading to ataxia and specific cerebellar lesions. Cell., 93(2):203-14.

Shun, C. T., Change, Y. C., Wu, H. P., Hsieh, S. C., Lin, W. M., Lin, Y. H., Tai, T. Y., and Hsieh, S. T. (2004). Skin denervation in type 2 diabetes: correlations with diabetic duration and functional impairments. Brain: a journal of neurology, 127(Pt 7):1593-605.

Sigurdson, C. (2018). Personal communication, unpublished data of novel 93N mouse model.

Sigurdson, C. J., Joshi-Barr, S., Bett, C., Winson, O., Manco, G., Schwarz, P., Rulicke, T., Nilsson, K. P. R., Ilan, M., Raeber, A., Peretz, D., Hornemann, S., Wuthrich, K., and Aguzzi, A. (2011). Spongiform encephalopathy in transgenic mice expressing a point mutation in the β2–α2 loop of the prion protein. The Journal of Neuroscience:

The Official Journal of the Society for Neuroscience, 31(39), 13840–13847. http://doi.org/10.1523/JNEUROSCI.3504-11.2011.

Sigurðsson B. Rida, (1954). A chronic encephalitis of sheep: with general remarks on infections which develop slowly and some of their special characteristics. British Veterinary Journal, 110:255–270.

Sima, A. A. F., Bouchier, M., and Christensen, H. (1983). Axonal atrophy in sensory nerves of the diabetic BB-Wistar rat: A possible early correlate of human diabetic neuropathy.

Solomon, I. H., Huettner, J. E., & Harris, D. A. (2010). Neurotoxic Mutants of the Prion Protein Induce Spontaneous Ionic Currents in Cultured Cells. The Journal of Biological Chemistry, 285(34), 26719–26726. http://doi.org/10.1074/jbc.M110.134619.

Sonati, T., Reimann, R. R., Falsig, J., Baral, P. K., O'Connor, T., Hornemann, S., Yaganoglu, S., Li, B., Herrmann, U. S., Wieland, B., Swayampakula, M., Rahman, M. H., Das, D., Kav, N., Riek, R., Liberski, P. P., James, M. N. G., and Aguzzi, A. (2013). The toxicity of antiprion antibodies is mediated by the flexible tail of the prion protein. Nature, 501:102-106.

Stahl, N., Baldwin, M. A., Hecker, R., Pan, K. M., Burlingame, A. L., and Prusiner, S. B. (1992). Glycosylinositol phospholipid anchors of the scrapie and cellular prion proteins contain sialic acid. Biochemistry, 31(21):5043-53.

Stahl, N., Borchelt, D. R., Hsaio, K., and Prusiner, S. B. (1987). Scrapie prion protein contains a phosphatidylinositol glycolipid. Cell, 51(2):229-40.

Stroobants, S., Gantois, I., Pooters T., and D'Hooge, R. (2013). Increased gait variability in mice with small cerebellar cortex lesions and normal rotorod performance. Behavioural Brain Research, 241:32-7. doi: 10.1016/j.bbr.2012.11.034.

Taveggia, C. (2016). Schwann cells-axon interaction in myelination. Cellular Neuroscience, 39:24-39. doi: 10.1016/j.conb.2016.03.006.

Taylor, T. N., Greene, J. G., & Miller, G. W. (2010). Behavioral phenotyping of mouse models of Parkinson's Disease. Behavioural Brain Research, 211(1), 1–10. http://doi.org/10.1016/j.bbr.2010.03.004.

Thackray, A. M., Hopkins, L., Klein, M. A., and Bujdoso, R. (2007). Mouse-adapted ovine scrapie prion strains are characterized by different conformers of PrPSc. Journal of Virology, 81(22):12119-12127. doi: 10.1128/JVI.01434-07.

Themistocleous, A. C., Kennett, R., Husain, M., Palace, J., Mead, S., & Bennett, D. L. H. (2014). Late onset hereditary sensory and autonomic neuropathy with cognitive impairment associated with Y163X prion mutation. Journal of Neurology, 261(11), 2230–2233. http://doi.org/10.1007/s00415-014-7521-6.

Thompson, A., MacKay, A., Rudge, P., Lukic, A., Porter, M. C., Lowe, J., Collinge, J., Mead, S. (2014). Behavioral and psychiatric symptoms in prion disease. The American Journal of Psychiatry, (171(3):265-74. DOI: 10.1176/appi.ajp.2013.12111460.

Thomzig, A., Schulz-Schaeffer, W., Wrede, A., Wemheuer, W., Brenig, B., Kratzel, C., Lemmer, K., and Beekes, M. (2007). Accumulation of Pathological Prion Protein PrPsc in Animals with Experimental and Natural Scrapie. PLoS Pathogens, https://doi.org/10.1371/journal.ppat.0030066.

Torres, J.-M., Andréoletti, O., Lacroux, C., Prieto, I., Lorenzo, P., Larska, M., Baron, T., and Espinosa, J.-C. (2011). Classical Bovine Spongiform Encephalopathy by Transmission of H-Type Prion in Homologous Prion Protein Context. Emerging Infectious Diseases, 17(9), 1636–1644. http://doi.org/10.3201/eid1709.101403.

Tranchant, C., Geranton, L., Guiraud-Chaumell, C., Mohr, M., Warter, J. M. (1999). Basis of phenotypic variability in sporadic Creutzfeldt-Jakob disease. Neurology, 52(6):1244-9.

Trevitt, C. R. and Singh, P. N. (2003). Variant Creutzfeldt-Jakob disease: pathology, epidemiology, and public health implications. The American Journal of Clinical Nutrition, 78(3):651S-656S, https://doi.org/10.1093/ajcn/78.3.651S.

Tribouillard-Tanvier, D., Race, B., Striebel, J. F., Carroll, J. A., Phillips, K., & Chesebro, B. (2012). Early Cytokine Elevation, PrPres Deposition, and Gliosis in Mouse Scrapie: No Effect on Disease by Deletion of Cytokine Genes IL-12p40 and IL-12p35. Journal of Virology, 86(19), 10377–10383. http://doi.org/10.1128/JVI.01340-12.

Turnbaugh, J. S., Unterberger, U., Saa, P., Massignan, T., Fluharty, B. R., Bowman, F. P., Miller, M. B., Supattapone, S., Biasini, E., and Harris, D. A. (2012). The N-terminal, polybasic region of PrPc dictates the efficiency of prion propagation by binding to PrPsc. The Journal of Neuroscience, 32(26):8817-8830.

Umeh, C. C., Kalakoti, P., Greenberg, M. K., Notari, S., Cohen, Y., Gambetti, P., Obla, A. L., Ghetti, B., and Mari, Z. (2016). Clinicopathological Correlates in a PRNP P102L Mutation Carrier with Rapidly Progressing Parkinsonism-dystonia. Movement Disorders Clinical Practice, 3(4), 355–358. http://doi.org/10.1002/mdc3.12307.

Villalon, E., Barry, D. M., Byers, N., Frizzi, K., Jones, M. R., Landayan, D. S., Dale, J. M., Downer, N. L., Calcutt, N. A., and Garcia, M. L. (2018). Internode length is reduced during myelination and remyelination by neurofilament medium phosphorylation in motor axons. Experimental neurology. 306:158-168. doi : 10.1016/j.expneurol.2018.05.009.

Von Hehn, C. A., Baron, R., & Woolf, C. J. (2012). Deconstructing the Neuropathic Pain Phenotype to Reveal Neural Mechanisms. Neuron, 73(4), 638–652. http://doi.org/10.1016/j.neuron.2012.02.008.

Wadsworth JD, Joiner S, Hill AF, Campbell TA, Desbruslais M, Luthert PJ, and Collinge J. (2001). Tissue distribution of protease resistant prion protein in variant Creutzfeldt-Jakob disease using a highly sensitive immunoblotting assay. Lancet, 358:171–80.

Wang, H., Cohen, M., Safar, J., Appleby, B. (2018). Peripheral neuropathy in patients with prion disease (p1.175). Journal of Neurology. 90(15 supplement) P1.175.

Watts, J. C., and Westaway, D. (2007). The prion protein family: diversity, rivalry, and dysfunction. Biochim Biophys Acta. 1772(6):654-72.

Watts, J. C., Giles, K., Patel, S., Oehler, A., DeArmond, S. J., Prusiner, S. B., DeArmond, S. J., Prusiner, S. B. (2014). Evidence that bank vole PrP is a universal acceptor for prions. Plos Pathog., 10:e1003990, doi: 10.1371/journal.ppat.1003990.

Waxman, S. G. (1975). Integrative properties and design principles of axons. Int Rev Neurobiol. 18():1-40.

Waxman, S. G. (1980). Determinants of conduction velocity in myelinated nerve fibers. Muscle Nerve, 3(2):141-50.

Weissman, C. (2004). The state of the prion. Nat Rev Microbiol., 2(11):861-71.

Weissmann, Charles & Flechsig, Eckhard. (2003). PrP knock-out and PrP transgenic mice in pion research. British medical bulletin. 66. 43-60. 10.1093/bmb/66.1.43.

Wells, G., Scott, A., Johnson, C., Gunning, R., Hancock, R., Jeffrey, M., Dawson, M., Bradley, R. (1987) A novel progressive spongiform encephalopathy in cattle. Veterinary Record, 121:419-420.

Westergard, L., Turnbaugh, J. A., Harris, D. A. (2011). A naturally occurring C-terminal fragment of the prion protein (PrP) delays disease and acts as a dominant-negative inhibitor of PrPSc formation. Journal of Biological Chemistry, 286(51):44234-42.

Will, R. G., Ironside, J. W., Zeidler, M., Cousens, S. N., Estiberio, K., Alperovitch, A., Poser, S., Pocchiari, M., Hofman, A., and Smith, P. G. (1996). A new variant of Creutzfeldt-Jakob disease in the UK. Lancet, 347(9006):921-5.

William, E. S. and Young, S. (1980). Chronic wasting disease of captive mule deer: a spongiform encephalopathy. J Wildl Dis, 16:89-98.

Wong, M, Jeng, A. Y. (1994). "Posttranslational modification of glycine-extended substance P by an alpha-amidating enzyme in cultured sensory neurons of dorsal root ganglia". Journal of Neuroscience Research. 37 (1): 97–102. doi:10.1002/jnr.490370113. PMID 7511706.

Wu, B., McDonald, A. J., Markham, K., Rich, C. B., McHugh, K. P., Tatzelt, J., Milhauser, G. L., Colby, D. W., and Harris, D. A. (2017). The N-terminus of the prion protein is a toxic effector regulated by the C-terminus. eLife, 6, e23473. http://doi.org/10.7554/eLife.23473.

Wu, L. M. N., Williams, A., Delaney, A., Sherman, D. L., & Brophy, P. J. (2012). Increasing Internodal Distance in Myelinated Nerves Accelerates Nerve Conduction to a Flat Maximum. Current Biology, 22(20), 1957–1961. http://doi.org/10.1016/j.cub.2012.08.025.

Wulf, M.-A., Senatore, A., & Aguzzi, A. (2017). The biological function of the cellular prion protein: an update. BMC Biology, 15, 34. http://doi.org/10.1186/s12915-017-0375-5.

Wuthrich, K., and Riek, R. (2001). Three-dimensional structures of prion proteins. Adv Protein Chem., 57():55-82.

Yagihashi, S., Kamijo, M., & Watanabe, K. (1990). Reduced myelinated fiber size correlates with loss of axonal neurofilaments in peripheral nerve of chronically streptozotocin diabetic rats. The American Journal of Pathology, 136(6), 1365–1373.

Yamakawa, Y., Hagiwara, K., Nohtomi, K., Nakamura, Y., Nishijima, M., Higuchi, Y., Sato, Y., Sata, Y., Expert Committee for BSE Diagnosis, Ministry of Health, Labour and Welfare of Japan. (2003). Atypical proteinase K-resistant prion protein (PrPres) observed in an apparently healthy 23-month-old Holstein steer. Japan Journal of Infectious Disease, 56(5-6):221-2.

Yang, W., Cook, J., Rassbach, B., Lemus, A., DeArmond, S. J., & Mastrianni, J. A. (2009). A New Transgenic Mouse Model of Gerstmann Sträussler Scheinker syndrome due to the A117V Mutation of PRNP. The Journal of Neuroscience : The Official Journal of the Society for Neuroscience, 29(32), 10072–10080. http://doi.org/10.1523/JNEUROSCI.2542-09.2009.

Yanguags-Casas, N. (2017). Sex differences in neurodegenerative diseases. SMGroup Journal of Neurological Disorders and Stroke, 3(1):1014.

Yoshikawa, D., Yamaguchi, N., Ishibashi, D., Yamanaka, H., Okimura, N., Yamaguchi, Y., Mori, T., Miyata, H., Shigematsu, K., Katamine, S., and Sakaguchi, S. (2008). Dominant-negative effects of the N-terminal half of prion protein on Neurotoxicity of Prion Protein-Like Protein/Doppel in Mice. Journal of Biological Chemistry, doi: 10.1074/jbc.M804212200.

Zahn, R., Liu, A., Luhrs, T., Riek, R., von Schroetter, C., Lopez Garcia, F., illeter, M., Calzolai, L., Wider, G., Wuthrich, K. (2000). NMR solution structure of the human prion protein. Proc Natl Acad Sci U S A., 97(1):145-50.

Zhang, Z., Zhang, Y., Wang, F., Wang, X., Xu, Y., Yang, H., Yu, G., Yuan, C., and Ma, J. (2013). FASEB, 27(12):4768-75.

Zochodne, D. W., Sun, H.-S., Cheng, C., and Eyer, J. (2004). Accelerated diabetic neuropathy in axons without neurofilaments. Brain, 127, 2193-2200.